Constraining Cosmological Parameters using Angular Diameter Distances of Galaxy Clusters

T H Anishya

MS12081

A dissertation submitted for the partial fulfilment of BS-MS dual degree in Science

Indian Institute of Science Education and Research Mohali

April 2017

Certificate of Examination

This is to certify that the dissertation titled **"Constraining Cosmological Parameters using Angular Diameter Distances of Galaxy clusters"** submitted by **T H Anishya** (Reg. No. MS12081) for the partial fulfilment of BS-MS dual degree programme of the Institute, has been examined by the thesis committee duly appointed by the Institute. The committee finds the work done by the candidate satisfactory and recommends that the report be accepted.

Prof Jasjeet Singh Bagla Dr Smriti Mahajan Dr H K Jassal

(Supervisor)

Dated:

Declaration

The work presented in this dissertation has been carried out by me under the guidance of Dr. H K Jassal at the Indian Institute of Science Education and Research, Mohali. This work has not been submitted in part or in full for a degree, a diploma, or a fellowship to any other university or institute. Whenever contributions of others are involved, every effort has been made to indicate this clearly, with due acknowledgement of collaborative research and discussions. This thesis is a bonafide record of original work done by me and all sources listed within have been detailed in the bibliography.

T H Anishya

MS12081

Dated: April 21, 2017

In my capacity as the supervisor of the candidate's project work, I certify that the above statements by the candidate are true to the best of my knowledge.

Dr H K Jassal

(Thesis Supervisor).

Acknowledgement

First and foremost, I would like to thank my thesis supervisor Dr H K Jassal, without whose supervision and guidance, this thesis would have never been possible. The discussions that I had with her has enhanced my capabilities at a professional level. I would also like to thank my thesis committee members Prof J S Bagla and Dr Smriti Mahajan for their valuable suggestions and criticism of my work.

I am highly grateful to the Deputy librarian, Dr Vishaki and Library Information Assistant Mr Shameer K. K. for their promptness and assistance.

I am thankful to IISER Mohali for providing the infrastructure and the Computer Centre for all the technical support. I would like to acknowledge DST INSPIRE, the Government of India for the financial support.

Finally, I would like to thank my family and friends for supporting and motivating me during the entire period of the project. I am also thankful to my seniors especially Archana Sangwan, for her useful advice and help.

T H Anishya

List of Figures

Contents

Abstract

Galaxy clusters are the most massive astrophysical objects bound by gravity. As the name suggests, these are groups of few tens to up to thousands of galaxies along with the intracluster medium and dark matter. These structures observable in optical, X-ray and radio wavelengths. Besides being of astrophysical importance, galaxy clusters prove to be reliable cosmological probes and can be used to understand the expansion history of the Universe, and provide insights into questions such as the nature of cosmic acceleration and growth rate. These are complementary to distance based probes such as Type Ia Supernovae and Baryon Acoustic Oscillations. The distribution of masses and redshift depend on the structures in the universe. Studies have demonstrated that Galaxy clusters using X-ray and Sunyaev Zel'dovich Effect(SZE) observations are potential probes of cosmology. Angular Diameter Distance(ADD) for galaxies derived from these observations are used as distance probes, that can be compared with theoretical models of cosmology and constrain the cosmological parameters.

In this thesis, I attempt to constrain the cosmological parameters governing the geometry and evolution of the Universe using galaxy clusters as distance probes and calculating their angular diameter distances using X-ray and SZE observations of different clusters. I will start by introducing different contesting cosmological models for the Universe, then describe the processes responsible for X-ray emission and SZE and the calculation of angular diameter distance from X-ray and SZE observations. I also discuss the mathematical tools required for model selection and lastly, I study the cosmological tests along with the effect of differently modelled morphologies of galaxy clusters on cosmological tests.

Chapter 1

Introduction

The Cosmological Principle assumes that the universe is homogeneous and isotropic. Along with the Weyl's postulate that stipulates that for a fluid cosmological model, the existence of a preferred coordinate system that is comoving with the background expansion flow. It reasoned that the universe is expanding on large scales and this evolution is a time-ordered sequence of the 3-d space which follows the cosmological principle. In the comoving frame, the large scale patterns stay the same. As the universe expand, we don't see the expansion effects. However, the physical distance between two points in such an expanding universe, which is a function of time, is proportional to the comoving distance, a constant in time. According to the Weyl's Postulate $R(t) = a(t)r$ where $R(t)$ is the proper distance between two points on the spacetime and r is the constant comoving distance and $a(t)$ is a universal function dependent only on time. This leads to the famous Hubble Law, i.e, $\dot{R} = HR$, where the Hubble parameter,

$$H = \frac{\dot{a}}{a}$$

1.1 Friedmann Universe

The Friedmann model, also called as the Friedmann-Lemaitre-Robertson-Walker model (FLRW model) is often referred to as the standard model of cosmology. This model uses Einstein's General Theory of Relativity with the Cosmological Principle to define the space-time and its dynamics.

As discussed earlier, the cosmological principle states that the universe is homogeneous and isotropic (at large scales) and forms the basis of the simple models of space-time. This simple coordinate system is valid for a class of observers for whom the universe is isotropic. To define such a coordinate system (t, x^α), the space-time interval ds^2 can be written as:

$$ds^2 = g_{ik}dx^i dx^k = g_{00}dt^2 + 2g_{0\alpha}dtdx^\alpha - \sigma_{\alpha\beta}dx^\alpha dx^\beta \tag{1.1}$$

where $\sigma_{\alpha\beta}dx^\alpha dx^\beta$ is a positive definite space metric. Assumption of isotropy implies that $g_{0\alpha}dtdx^\alpha$ must vanish and using natural units, i.e, $h = c = 1$, $g_{00} = 1$, which makes the space-time interval as:

$$ds^2 = dt^2 - \sigma_{\alpha\beta}dx^\alpha dx^\beta \equiv dt^2 - dl^2 \tag{1.2}$$

Now, Isotropy implies spherical symmetry at all times, therefore the space interval following spherical symmetry can be defined as:

$$dl^2 = a^2[\lambda^2(r)dr^2 + r^2(d\theta^2 + sin^2\theta d\phi^2)] \tag{1.3}$$

where $a = a(t)$ can be the only variable dependent on time. The scalar curvature of three-dimensional spherically symmetric space is:

$${}^3R = \frac{3}{2a^2r^3}\frac{d}{dr}\left[r^2\left(1 - \frac{1}{\lambda^2}\right)\right] \tag{1.4}$$

For a homogeneous space, the curvature must be a constant k',i.e,

$$1 - \frac{1}{\lambda^2} = kr^2$$

where $k = 2a^2k'$ which gives the space-time metric as:

$$ds^2 = dt^2 - a^2(t)\left[\frac{dr^2}{1 - kr^2} + r^2(d\theta^2 + sin^2\theta d\phi^2)\right] \tag{1.5}$$

To simplify the representation of this metric, we define a coordinate χ as

$$\chi = \int \frac{dr}{\sqrt{1 - kr^2}}$$

The metric can be written in terms of (χ, θ, ϕ) as:

$$dl^2 = a^2[d\chi^2 + S_k^2(\chi)(d\theta^2 + sin^2\theta d\phi^2)] \tag{1.6}$$

where,

$$S_k(\chi) = \begin{cases} \sin\chi & \text{for } k = +1 \\ \chi & \text{for } k = 0 \\ \sinh\chi & \text{for } k = -1 \end{cases}$$

Friedmann universe can have positive, zero and negative curvatures ($k = +1, 0, -1$) which indicate spatially open, flat and closed universes respectively.

1.1.1 Kinematics of the Friedmann Model

The proper distance between two spatial points changes in time in proportion to the scale factor $a(t)$ such that the proper distance is defined as:

$$l(t) = l_0 a(t) \tag{1.7}$$

where l_0 is the comoving distance.

The velocity of an object as seen by an observer with proper distance l to the object is

$$\delta v = \frac{dl}{dt} = \dot{a} l_0 = \frac{\dot{a}}{a} l \tag{1.8}$$

If the two observers are moving with a relative velocity δv, and one observer encounters an electromagnetic radiation of frequency ω, they will observe, that the frequency of the radiation, as received by the second observer is doppler shifted and is $\omega + \delta\omega$, therefore,

$$\frac{\delta\omega}{\omega} = -\frac{\delta v}{c} = -\delta v \frac{\delta t}{l} \tag{1.9}$$

since $\delta v = \frac{\dot{a}}{a} l$,

$$\frac{\delta\omega}{\omega} = -\frac{\dot{a}}{a}\delta t = -\frac{\delta a}{a} \tag{1.10}$$

This equation can be integrated to find

$$\omega(t) a(t) = constant \tag{1.11}$$

These results indicate that the observed wavelength of radiation emitted by a source at time t_e and observed at a later time t_o depends on the value of scale factors a at

these two different times, $a(t_e)$ and $a(t_o)$ respectively. In an expanding phase, i.e, $a(t_o) > a(t_e)$, the wavelength is redshifted, such that

$$1 + z(t) = \frac{a(t_o)}{a(t)} = \frac{a_o}{a(t)} \tag{1.12}$$

Most cosmological observations are based on Electromagnetic waves which are emitted from far away sources and observed on Earth(or other satellites in space). These waves travel at velocity c and thus follow a null geodesic, i.e, $ds^2 = 0$. For a photon emitted by a source at r_{em} from the observer at the origin, at time t_e and is observed at time t_o, the path followed is

$$ds^2 = dt^2 - a^2(t)\frac{dr^2}{1 - kr^2} = 0 \tag{1.13}$$

Integrating the above equation gives,

$$\int_{t_e}^{t_o} \frac{dt}{a(t)} = \int_0^{r_{em}} \frac{dr}{\sqrt{1 - kr^2}} \tag{1.14}$$

differentiating eq. 1.12 we can write,

$$dt = \frac{-a(t)^2}{a(t_o)\dot{a}}dz \tag{1.15}$$

$$\frac{dt}{a(t)} = \frac{-a(t)}{a(t_o)\dot{a}}dz \tag{1.16}$$

Hence, the above integral (eq. 1.14) can be written as a function of redshift z instead of time t. The radial distance r_{em} which gives the radial distance to the source from the observer can be written as a function of redshift. Such a relation is of importance to cosmological observations as it provides the epoch in which the observed light is emitted. To determine the relation of r_{em} with redshift z, we define Hubble radius d_H as

$$d_H(t) = d_H(z) = \frac{a}{\dot{a}} \tag{1.17}$$

Integrating the above equation and writing the right-hand side as $S_k^{-1}(x) = [sinh^{-1}(x), x, sin^{-1}(x)]$ for $k = -1, 0$ and $+1$ respectively we get:

$$\frac{1}{a_o}\int_0^z d_H(z)dz = S_k^{-1}(r_{em}) \tag{1.18}$$

$$\Rightarrow r_{em}(z) = S_k(\alpha), \text{where } \alpha = \frac{1}{a_o}\int_0^z d_H(z)dz \tag{1.19}$$

The radial distance to source plays a role in two important observable quantities: luminosity or flux and the angular size of the source.

The flux F observed from a source of luminosity L is described as

$$F = \frac{L}{(area)} = \frac{L}{4\pi a^2 r_{em}^2} = \frac{L}{a\pi a_o^2 r_{em}^2 (1+z)^2} \tag{1.20}$$

Thus the Luminosity distance, distance to the objects with luminosity L and flux F can be defined as

$$d_L(z) = \sqrt{\frac{L}{a\pi F}} = a_o r_{em}(z)(1+z) = a_o(1+z)S_k(\alpha) \tag{1.21}$$

The observed angular diameter or the angular size δ of the source of physical size D, and angular diameter distance d_A, is defined as

$$\delta = \frac{D}{d_A}$$

The angular diameter distance(d_A), thus describes the physical distance of the source from the observer and can be written as:

$$d_A = r_{em} a(t_e) = a_o r_{em}(t_e)(1+z)^{-1} \tag{1.22}$$

From eq. 1.21 and eq. 1.22 we get the relation:

$$d_L = (1+z)^2 d_A \tag{1.23}$$

1.1.2 Dynamics of the Friedmann Model

The evolution of the universe populated by different sources can be determined by the Einstein's equations from the General theory of Relativity,givenby

$$G_k^i = R_k^i - \frac{1}{2}\delta_k^i R = 8\pi G T_k^i \tag{1.24}$$

where T_k^i is the stress-energy tensor of the form

$$T_k^i = dia[\rho(t), -p(t), -p(t), -p(t)] \tag{1.25}$$

for ideal fluids and R_k^i and R are the Riccie tensor and scalar, respectively. Using the FLRW metric, G_k^i can be calculated to give the following equations, which are called the cosmological Equations.

$$\frac{\dot{a}^2 + k}{a^2} = \frac{8\pi G}{3}\rho \tag{1.26}$$

$$\frac{2\ddot{a}}{a} + \frac{\dot{a}^2 + k}{a^2} = -8\pi G p \tag{1.27}$$

From eq. 1.26,

$$\frac{k}{a^2} = \frac{8\pi G}{3}\rho - \frac{\dot{a}^2}{a^2} \tag{1.28}$$

$$= \frac{\dot{a}^2}{a^2}\left[\frac{\rho}{3H^2/8\pi G} - 1\right] \tag{1.29}$$

where $H(t) \equiv \frac{\dot{a}}{a}$. This clearly implies that if $\rho > 3H^2/8\pi G$ that the curvature of the space-time would be positive and if $\rho < 3H^2/8\pi G$ the curvature would be negative. For a flat universe, the curvature $k = 0$, the critical density which achieves this condition is given by

$$\rho_c(t) \equiv \frac{3H^2}{8\pi G} \tag{1.30}$$

Therefore, the eq. 1.28 at $t = t_o$ can be written as,

$$\frac{k}{a^2} = H_o^2(\Omega - 1) \tag{1.31}$$

Where $\Omega \equiv \Omega(t) \equiv \frac{\rho}{\rho_c}$ is called the density parameter.
Substituting from eq. 1.31 to the second Friedmann equation, eq. 1.27, gives,

$$\frac{\ddot{a}}{a} = -\frac{4\pi G}{3}(\rho + 3p) \tag{1.32}$$

To solve these equations explicitly, from eq. 1.26 we get,

$$\rho a^3 = \frac{3}{8\pi G}a(\dot{a}^2 + k) \tag{1.33}$$

Differentiating the above equation with respect to the scale factor a gives,

$$\frac{d(\rho a^3)}{da} = \frac{3a^2}{8\pi G}\left(\frac{(\dot{a}^2 + k)}{a^2} + \frac{2\ddot{a}}{a}\right) \tag{1.34}$$

Substituting from eq. 1.32 we get,

$$\frac{d(\rho a^3)}{da} = -3a^2 p \tag{1.35}$$

For an equation of state $\rho = \omega p$,which is the equation of state for isotropic fluid, the above equation gives,

$$\frac{d(\rho a^3)}{da} = -3a^2\omega\rho \tag{1.36}$$

Integrating the above equation gives,

$$\rho \propto a^{-3(1+\omega)} \tag{1.37}$$

Thus, for non-relativistic matter $\rho \propto a^{-3}$ as $\omega = 0$, for radiation $\omega = 1/3$ and $\rho \propto a^{-4}$. For $\omega = -1$, $\rho \propto a^0$(constant) and $\rho = -p$, i.e, negative pressure and the universe expands since $\frac{\dot{a}}{a} > 0$.

From eq. 1.33, we can write $(\dot{a}^2/a^2) \propto a^{-3(1+\omega)}$ or $\dot{a}^2 \propto a^{-\frac{1}{2}(1+3\omega)}$, integrating which, we get

$$a(t) \propto \begin{cases} t^{\frac{2}{3(1+\omega)}} & \text{for } \omega \neq -1 \\ exp(\lambda t) & \text{for } \omega = -1 \\ t^{2/3} & \text{for } \omega = 0 \\ t^{1/2} & \text{for } \omega = 1/3 \\ t^{1/3} & \text{for } \omega = 1 \end{cases} \tag{1.38}$$

Now, the total energy density can be written as:

$$\rho_{tot}(a) = \rho_R(a) + \rho_{NR}(a) + \rho_V(a) \tag{1.39}$$

where ρ_R, ρ_{NR} and ρ_Λ indicate the densities of radiation, non-relativistic matter and dark energy in the universe. The total energy density can thus, be written as:

$$\rho_{tot}(a) = \rho_c \left[\Omega_R \left(\frac{a_o}{a} \right)^4 + \Omega_{NR} \left(\frac{a_o}{a} \right)^3 + \Omega_\Lambda \right] \tag{1.40}$$

Substituting the above equation in the Friedmann equation gives:

$$\frac{\dot{a}^2}{a^2} + \frac{k}{a^2} = H_o^2 \left[\Omega_R \left(\frac{a_o}{a} \right)^4 + \Omega_{NR} \left(\frac{a_o}{a} \right)^3 + \Omega_\Lambda \right] \tag{1.41}$$

As the total density parameter should be 1 for a flat universe, we can write $\frac{k}{a^2} = (\Omega - 1) H_o^2 (a_o/a)^2$ to account for the curvature, where Ω is the total density parameter. Defining $\tau = H_o t$ and $a = a_o q(t)$ and substituting it in eq. 1.41 gives:

$$\left(\frac{da}{d\tau} \frac{H_o}{a} \right)^2 = H_o^2 \left[\Omega_R \left(\frac{a_o}{a} \right)^4 + \Omega_{NR} \left(\frac{a_o}{a} \right)^3 - (\Omega - 1) \left(\frac{a_o}{a} \right)^2 + \Omega_\Lambda \right] \tag{1.42}$$

$$\left(\frac{dq}{d\tau} \right)^2 = \left[\frac{\Omega_R}{q^2} + \frac{\Omega_{NR}}{q} - (\Omega - 1) + \Omega_\Lambda q^2 \right] \tag{1.43}$$

This can be written as:

$$\frac{1}{2}\left(\frac{dq}{d\tau}\right)^2 + V(q) = E \tag{1.44}$$

where,

$$V(q) = -\frac{1}{2}\left(\frac{\Omega_R}{q^2} + \frac{\Omega_{NR}}{q} + \Omega_\Lambda q^2\right), E = \frac{1}{2}(1-\Omega) \tag{1.45}$$

Considering a matter dominated universe, i.e, Ω_Λ is zero and Ω_R is negligible, then eq. 1.42 can be integrated to give the solution:

$$H_o t = \frac{\Omega}{2(\Omega-1)^{3/2}}\left[cos^{-1}\left(\frac{\Omega z - \Omega + 2}{\Omega z + \Omega}\right) - \frac{2(\Omega-1)^{1/2}(\Omega z+1)^{1/2}}{\Omega(1+z)}\right] \tag{1.46}$$

for $\Omega > 1$ and,

$$H_o t = \frac{\Omega}{2(1-\Omega)^{3/2}}\left[\frac{2(1-\Omega)^{1/2}(\Omega z+1)^{1/2}}{\Omega(1+z)} - cosh^{-1}\left(\frac{\Omega z - \Omega + 2}{\Omega z + \Omega}\right)\right] \tag{1.47}$$

For a dark energy / cosmological constant dominated flat universe, i.e, $\Omega_V > \Omega_{NR}$, and $\Omega_{NR} + \Omega_\Lambda = 1$ the solution is

$$\left(\frac{a}{a_o}\right) = \left(\frac{\Omega_{NR}}{\Omega_\Lambda}\right)^{1/3} sinh^{2/3}\left(\frac{3}{2}\sqrt{\Omega_\Lambda} H_o t\right) \tag{1.48}$$

These equations completely define the scale factor $a(t)$. From eq 1.17, Hubble radius can be defined as

$$d_H(z) = H_o^{-1}[\Omega_R(1+z)^4 + \Omega_{NR}(1+z)^3 + (1-\Omega)(1+z)^2 + \Omega_\Lambda]^{-1/2} \tag{1.49}$$

From eq 1.22, we can calculate the angular diameter distance as

$$d_A = (1+z)^{-1}\int_0^z H_o^{-1}[\Omega_R(1+z)^4 + \Omega_{NR}(1+z)^3 + (1-\Omega)(1+z)^2 + \Omega_\Lambda]^{-1/2} dz \tag{1.50}$$

[1]

[1]For a more detailed discussion refer to Theoretical Astrophysics Vol III, T Padmanabhan[1]

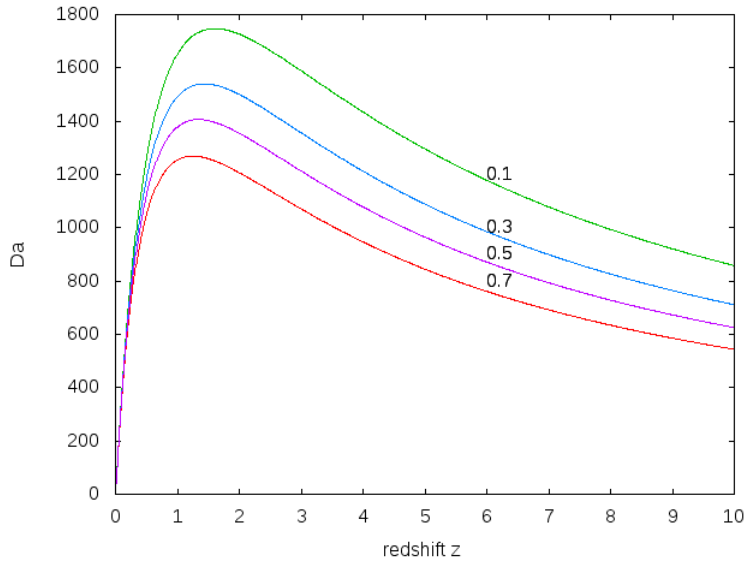

Figure 1.1: Angular diameter distance as a function of redshift for different values of $\Omega_m = 0.1, 0.3, 0.5, 0.7$ for a flat universe.

1.2 $R_H = ct$ universe

The gravitational radius of the universe that is defined as the radius containing all the mass combined with the Friedmann equation for flat universe can also be written as $R_H = c\frac{\dot{a}}{a}(Melia, 2012)[2]$. Combining Weyl's postulate $R_H = a(t)R_H$ with this we can write $R_H = ct$. The angular diameter distance in such a universe can thus be described as

$$d_A = (1+z)^{-1} \int_0^z R_H(z)dz \tag{1.51}$$

$$= (1+z)^{-1} \int_0^z \frac{1}{1+z}dz \tag{1.52}$$

$$d_A = \frac{c}{H_o}\frac{ln(1+z)}{(1+z)} \tag{1.53}$$

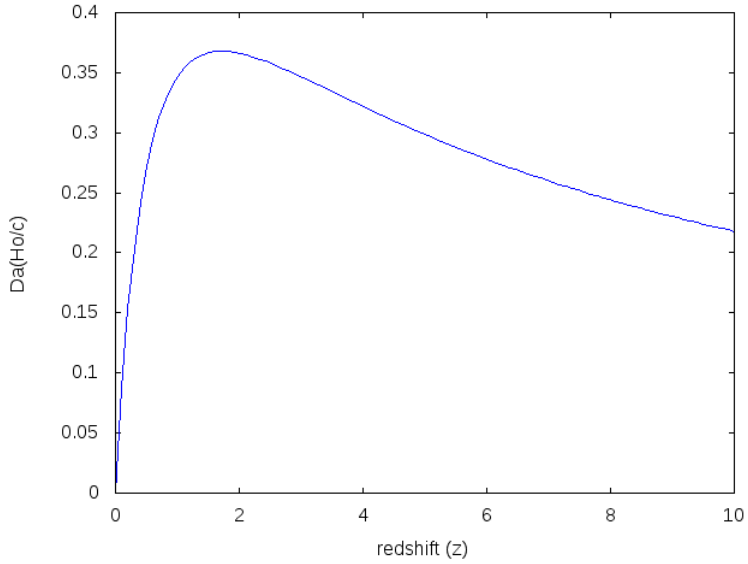

Figure 1.2: Angular diameter distance as a function of redshift for a flat universe following the $R_H = ct$ model.

Chapter 2

Determination of Cosmic Distances using SZE and X-ray

The intergalactic medium that occupies the space between galaxies in a cluster interacts with the X-ray and thermal cosmic background radiations(CBR). This interaction of diffuse matter($T_e \approx 10^7 - 10^8 K$) leaves a signature in the spectra of a cluster. Combined analysis of these radio and X-ray spectra can be used to derive directly the distances to these galaxy clusters. This method uses the Sunyaev-Zel'dovich Effect(SZE) and the emission of X-rays in galaxy clusters.

2.1 Sunyaev-Zel'dovich Effect

The CBR($T \approx 3K$) when passes through the hot diffuse plasma of the intracluster medium gets scattered by free electrons. The CBR photons are Thomson scattered by the hot electrons and produces visible effects in the CBR spectra. If the energy of the electrons is much larger than CBR photons, doppler shift is introduced in the scattered radiation. This effect is called the Sunyaev-Zel'dovich Effect(SZE).

2.1.1 Compton-Thomson Scattering

The electron-photon scattering reaction:

$$e + \gamma \longleftrightarrow e' + \gamma'$$

If the electron energy and the energy of photon were small, the scattering of such photons would produce only negligible deflection in the photon frequency and would not change the spectra observed. In such a case, the net rate of the reaction can be described as

$$\frac{dN}{dt} = A[N - N'] \tag{2.1}$$

where N and N' are respectively the total numbers of available photons on the left and right sides of the above mentioned reaction and A is the rate coefficient. Since the photon energies are small compared to the mass of electrons, electron recoil can be ignored. The integrated effect of many scatterings produces a random walk in photon energies and can produce an observable effect on the CBR spectra. This evolution of the spectrum of homogeneous and isotropic radiation being elastically scattered by a homogeneous gas of electrons is defined by Kompaneets equation[3]. To derive this equation, we assume a homogeneous and isotropic distribution of electron gas in the laboratory frame, $F1$ and the initial rest frame is indicated as F. The Lorentz transformation of electrons moving with speed v along the x-axis in $F1$ is:

$$t = \gamma(t_1 + vx_1) \qquad x = \gamma(x_1 + vt_1) \tag{2.2}$$

And the energy transformation of photons moving at an angle θ with the x-axis is given by:

$$\nu = \gamma\nu_1(1 + vcos\theta_1) \qquad \nu cos\theta = \gamma\nu_1(cos\theta_1 + v) \tag{2.3}$$

and the energy transformation the other way around is given by:

$$\nu_1 = \gamma\nu(1 - vcos\theta_1) \tag{2.4}$$

which gives:

$$\gamma(1 - vcos\theta_1) = \frac{1}{\gamma(1 + vcos\theta_1)} \tag{2.5}$$

and,

$$cos\theta = \frac{cos\theta_1 + v}{1 + vcos\theta_1} \tag{2.6}$$

which describes the transformation of the angle of motion of the photons. Differentiating with respect to θ the above equation would give the transformation of the solid angle ($d\Omega = dcos\theta d\theta$) of a beam of photons:

$$d\Omega = \frac{d\Omega_1}{\gamma^2(1 + vcos\theta_1)^2} \tag{2.7}$$

Now, $N_1 = N$ is the transformation law for the photon distribution as it is a scalar and would remain the same in both frames.

As the photons are assumed to be moving along the x-axis, net rate R_1 of scattering the photons into and out of the beam as observed in the rest frame of the electron is given by:

$$\frac{\partial N_1}{\partial t_1} + cos\theta_1 \frac{\partial N_1}{\partial x_1} = R_1 \tag{2.8}$$

From the above two equations, we get

$$\frac{\partial N_1}{\partial t_1} = \gamma \frac{\partial N}{\partial t} \qquad \frac{\partial N_1}{\partial x_1} = \gamma v \frac{\partial N}{\partial x} \tag{2.9}$$

Hence,

$$\gamma \frac{\partial N}{\partial t}(1 + vcos\theta_1) = R_1 \tag{2.10}$$

Using eq 2.5 we get,

$$\frac{\partial N}{\partial t} = \langle \gamma(1 - vcos\theta) R_1 \rangle_\theta \tag{2.11}$$

After scattering, the momentum of electron in the electron rest frame is

$$m v_1' = \vec{\nu_1} - \vec{\nu_1'} \tag{2.12}$$

The final kinetic energy of the electron, which is equal to the energy lost by the photon gives the Compton shift:

$$\nu_1 - \nu_1' = \delta\nu_1 = \frac{\nu_1^2}{m}(1 - cos\theta) \tag{2.13}$$

And the rate of change of number of photons in a beam element of solid angle $d\Omega_1$ and range of frequency $\nu_1 to \nu_1 + d\nu_1$ is given by

$$R_1 \nu_1^2 d\nu_1 d\Omega_1 = \frac{d}{dt_1} N_1(\theta_1, \nu_1) \nu_1^2 d\nu_1 d\Omega_1 = \int \frac{d\sigma}{\Omega_s} I, \tag{2.14}$$

where $\frac{d\sigma}{\Omega_s}$ is the cross section of scattering and I is the rate of scattering of photons into the beam element minus the rate of photons scattered out of the beam. From eq. 2.3 the Compton shifted photon energy can be written as:

$$\nu^{\pm} = \nu_1^{\pm} \gamma(1 + vcos\theta_1') \tag{2.15}$$

$$= \nu \frac{\nu_1^{\pm}}{\nu_1} \frac{(1 + vcos\theta_1')}{1 + vcos\theta_1} \tag{2.16}$$

where $\nu^{\pm} = \nu \pm d\nu$ and expanding v^2 and ν/m, we get,

$$\nu^{\pm} = \nu[1 \pm (\nu/m)(1 - cos\theta) + v(cos\theta_1' - cos\theta_1) + v^2(cos^2\theta_1 - cos\theta_1' cos\theta_1)] \quad (2.17)$$

From eq. 2.16, The momentum volume element form the rate of scattering of photons into the beam element in I, can be written as:

$$\left\langle \nu_1^+ \right\rangle^2 d\nu_1^+ = \left[1 + 4\frac{\nu_1}{m}(1 - cos\theta)\right] \nu_1^2 d\nu_1 \quad (2.18)$$

From eq. 2.10 and eq. 2.14, we can write the equation for the rate of collision as

$$\frac{\partial N}{\partial t} = \int \gamma(1 - vcos\theta)\frac{d\Omega}{4\pi}\frac{d\sigma}{d\Omega_s} d\Omega_1'(A + B) \quad (2.19)$$

where $A = \frac{4\nu}{m}(1 - cos\theta)N\nu[1 + N\nu]$ and $B = [1 + N\nu]N(\nu + \Delta^+) - [1 + N(\nu + \Delta^-)]N\nu$ By expanding B in $\Delta^{\pm}$ and rearranging, and keeping terms till first order in ν we can write

$$\frac{\partial N}{\partial t} = \int (1 - 3vcos\theta_1)\frac{d\Omega_1}{4\pi}\frac{d\sigma}{d\Omega_s} d\Omega_1'(A + B) \quad (2.20)$$

Using classical Thomson cross-section, we can write

$$\frac{\partial N}{\partial t} = \sigma_t C$$

Where C is the expectation value calculated for scattering by a single electron:

$$C = \frac{\nu}{m}\left[4N(1 + N) + (1 + 2N)\nu\frac{dN}{d\nu}\right] + \frac{4}{3}\frac{dN}{d\nu}\nu v^2 + \frac{1}{3}\frac{d^2N}{d\nu^2}\nu^2 v^2$$

The Kompaneets equation thus becomes:

$$\frac{1}{\sigma_t n_e}\frac{\partial N}{\partial t} = \frac{\nu}{m}\left[4N(1 + N) + (1 + 2N)\nu\frac{dN}{d\nu}\right] + \frac{4}{3}\frac{\partial N}{\partial \nu}\nu\left\langle v^2 \right\rangle + \frac{1}{3}\frac{\partial^2 N}{\partial \nu^2}\nu^2\left\langle v^2 \right\rangle \quad (2.21)$$

If the electrons have a Maxwell-Boltzmann distribution for energy at temperature T_e, then the dispersion relation can be written as:

$$\left\langle \nu^2 \right\rangle = 3kT_e/m_e$$

Using scaled variable $x = \frac{h\nu}{kT_e}$, $dy = \frac{kT_e}{m_e c^2}\sigma_t n_e c dt$, eq. 2.21 can be written as

$$\frac{\partial N}{\partial y} = x^2\frac{\partial^2 N}{\partial x^2} + (x^2 + 4x + 2x^2 N)\frac{\partial N}{\partial x} + 4xN(1 + N) \quad (2.22)$$

where $y = \frac{k\langle T_e \rangle}{m_e c^2} \int^t \sigma_t n_e c dt$.

Since the plasma in ICM is much hotter than CMBR, $x << 1$. In this limit, eq. 2.22 can be written as:

$$\frac{\partial N}{\partial y} = \nu^2 \frac{\partial^2 N}{\partial \nu^2} + 4\nu \frac{\partial N}{\partial \nu} \tag{2.23}$$

Since the CMBR is approximately like a black body spectrum, the occupation number can be written as

$$N = \frac{1}{e^{h\nu/kT} - 1}$$

we can write in the limit $x << 1$:

$$\frac{\delta N}{N} = -2y$$

, In Rayleigh-Jeans approximation $N \propto T$, we get the temperature decrement as:

$$\frac{\delta T}{T} = -2 \frac{k \langle T_e \rangle}{m_e c^2} \int^t \sigma_t n_e c dt \tag{2.24}$$

2.2 X-Ray Emission in Cluster of Galaxies

X-ray emission in the galaxy clusters was first discovered in the Coma and Perseus clusters and proved that the space between the galaxies in a cluster was occupied by extremely hot($\approx 10^8 K$), low density($\approx 10^{-3} n_e / cm^{-3}$) ionised gas which was termed as the Intra cluster medium(ICM). Thermal bremsstrahlung was suggested by Felten et al.(1966)[4] as the phenomena that caused X-ray emission from the cluster plasma.

2.2.1 Thermal Bremsstrahlung from ICM

At the physical conditions of ICM($T \approx 10^8 K$ and $\approx 10^{-3} n_e / cm^{-3}$), the primary emission process from the cluster plasma (constituted mainly of hydrogen) is free-free emission of thermal bremmstrahlung, and hence is the main cooling process for high temperature plasma. The emissivity at a particular frequency ν is given by:

$$e_\nu^{ff} = \frac{2^5 \pi e^6}{3 m_e c^3} \left(\frac{2\pi}{3 m_e K_b} \right)^{1/2} Z^2 n_e n_i g_{ff}(Z, T_g, \nu) T_g^{-1/2} e^{\frac{-h\nu}{K_b T_g}} \tag{2.25}$$

where Z is the charge of the ion, T_g is the temperature of the gas, n_i and n_e are the number densities of ions and electrons respectively and g_{ff} is the gaunt factor (Sarazin 1988[5]). Observations indicate that the cluster plasma fits fairly well to this equation at gas temperature 10^7 to $10^8 K$ which indicates that the emission decreases exponentially with an increase in frequency.

The cooling coefficient, Λ_{eH} is defined as the integral of emissivity over all frequencies:

$$\Lambda_{eH} = \int e_\nu^{ff} d\nu$$

The elastic coulomb collisions between the ions and elctrons in the plasma has a time scale much lower than the age of the plasma and these particles follow a Maxwell-Bolzmann distribution at high temperatures which determines the rates of excitations and ionization processes. So the X-ray surface brightness of clusters depend upon the gass mass distribution and the emissivity integrated over all frequencies, i.e, the cooling coefficient. The surface brightness is thus defined as:

$$S_x \propto \int_{LOS} n_e^2 \Lambda_{eH} dl$$

2.3 Angular Diameter Distance from SZE and X-Ray observations

We have seen in the earlier sections that the measured temperature decrement ΔT arising from SZE and the measure of X-ray surface brightness S_x depend on the distribution of cluster gas and thus the cluster morphology. Hence, it is essential to build a model for the distribution of cluster gas which has a higher density at the centre, such that the radiative cooling time scale is lesser than the age of the cluster. This is suggested from the X-ray observations which show increased density at the cluster centre which decreases at a higher radius. For this, the isothermal β model suggested first by Cavalier and Fusco-Feriano(1976) [6] and later generalised into a double β model gave:

$$n_e(r) = n_{e0} \left[f \left(1 + \frac{r^2}{r_{c1}^2} \right)^{\frac{-3\beta}{2}} + (1-f) \left(1 + \frac{r^2}{r_{c2}^2} \right)^{\frac{-3\beta}{2}} \right] \tag{2.26}$$

where n_{eo} is the high central density, r_{c1} is radius of the core and r_{c2} is the outer radius of the cluster and β is the slope at large radii.

The measured temperature decrement of the CMB is given by:

$$\Delta T = T_{CMB} f(\nu, t_e) \frac{K_B \sigma_T}{m_e c^2} \int_{LOS} n_e T_e dl \tag{2.27}$$

where T_e is the temperature of ICM, $T_{CMB} = 2.728K$(Fixsen et al. 1996)[7], K_B, σ_T, m_e and c are the Boltzmann constant, Thomson cross section of the electron, the mass of electron and speed of light in vacuum respectively. $f(\nu, T_e)$ is the function which accounts for frequency shifts and relativistic corrections and is taken to be -2. The central temperature decrement resulting from the line of sight integration above equation is given by:

$$\Delta T = T_{CMB} f(\nu, T_e) \frac{K_B \sigma_T T_e}{m_e c^2} n_{eo} \sqrt{\pi} \frac{D_a \theta_c}{\sqrt{e_{proj}}} g(\beta/2) \tag{2.28}$$

, with

$$g(\alpha) = \frac{\Gamma(3\alpha - 1/2)}{\Gamma(2\alpha)} \tag{2.29}$$

where, D_a is the angular diameter distance, θ_c the projected angular position and e_{proj} is the projected eccentricity of the cluster.

The X-Ray surface brightness due to thermal bremsstrahlung and line emission gives X-ray surface brightness as

$$S_x = \frac{1}{4\pi(1+z)^4} \int_{LOS} n_e^2 \Lambda_{eH} dl \tag{2.30}$$

where Λ_{eH} is the X-ray cooling function of the intra cluster medium and z is the redshift of the cluster. The observed surface brightness obtainbed after the LOS integration with the isothermal β model of ICM plasma gives:

$$S_x = \frac{\Lambda_{eH}(\mu_e/\mu_H)}{4\sqrt{\pi}(1+z)^4} n_{eo}^2 \frac{D_c \theta_c}{\sqrt{e_{proj}}} g(\beta) \tag{2.31}$$

Combining eq 2.28 and eq.2.31 to eliminate the central electron density we obtain angular diameter distance as:

$$D_a = \frac{\Delta T^2}{S_x} \left(\frac{m_e c^2}{K_B T_{eo}} \right)^2 \frac{\Lambda_{eH}(\mu_e/\mu_H)}{4\pi^{3/2} f(\nu, T_e)^2 T_{CMB}^2 \sigma_T^2 (1+z)^4 \theta_c} \frac{g(\beta)}{g(\beta/2)^2} \tag{2.32}$$

The theoretical angular diameter distance can then be compared with the one obtained from observations.

Chapter 3

Optimisation of Parameters and Model Selection

In this work, we have used the χ^2 statistics for finding the best fit parameters and model selection tools such as Akaike Information Criterion(AIC) and Bayes Information Criterion(BIC)(Wei et al. (2014)[9]) are used for cosmological model comparison.

3.1 The χ^2 Distribution

This method of finding the best fit for a parameter (a) with a data of n points (t_j) uses the method of least square, wherein the weighted sum of squares of deviations is minimised; i.e,

$$\chi^2 = \sum_{j=1}^{n} \left(\frac{y_j - y(t_j, a, ..)}{\Delta y_j} \right)^2 \tag{3.1}$$

is minimised. In this method, the measurements with smaller Δy are given higher weight.

Each measurement or data point is represented as a random variable X with a normal probability distribution with mean zero and variance $\sigma^2 = 1$. The probability density of X is thus,

$$f(x) = \frac{1}{\sigma\sqrt{2\pi}} e^{-x^2\sigma^2} \tag{3.2}$$

The probability density of a random variable $Y = X^2$, which takes positive values will be zero if $y \leq 0$. Thus, the probability distribution for Y can be written as:

$$g(y) = \frac{d}{dy}[P(\sqrt{y}) - P(-\sqrt{y})] = \frac{1}{2\sqrt{y}}(f(\sqrt{y}) + f(-\sqrt{y}))$$

$$= \frac{1}{\sigma\sqrt{2\pi y}} e^{-y/2\sigma^2} \tag{3.3}$$

The goodness of fit is assessed by the random variable $Y = \sum_{y=1}^{n} X_j^2$ where n is the number of degree of freedom. $n = N - r$ for N measured data points and r parameters that are to be fitted. The probability density of this random variable can be written in the form of gamma distribution:

$$g_n(y) = \frac{y^{n/2-1}}{2^{n/2}\sigma^n \Gamma(n/2)} e^{-y/2\sigma^2} \tag{3.4}$$

From eq. 3.3 the mean and variance of the random variable Y is

$$\langle Y \rangle = n\sigma^1$$

and

$$\sigma^2(Y) = 2n\sigma^4$$

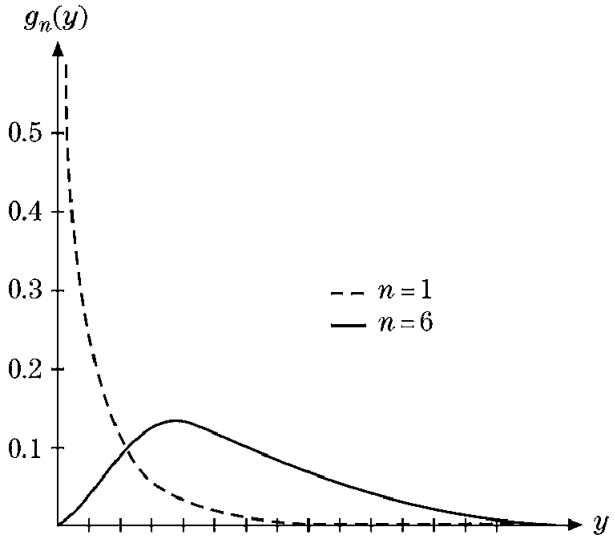

Figure 3.1: χ^2 Probability density[10]

And the probability distribution of χ^2 with n degrees of freedom can be written as the integral of eq. 3.4 as:

$$P(\chi^2 \geq y_o) = \frac{1}{2^{n/2}\sigma^n \Gamma(n/2)} \int_{y_o}^{\infty} y^{n/2-1} e^{-y/2\sigma^2} dy \tag{3.5}$$

The confidence interval is thus, the interval in the parameter space, in which the probability that the unknown parameter lies in the interval is high or of a given probability.

3.2 Model Selection Tools

In this study, we use model selection tools such as Akaike Information Criteria(AIC) and Bayesian Information Criteria(BIC) in conjunction with maximum likelihood has been used for finding the best model of cosmology fitting the observed data. Use of model selection tools for cosmological parameter fitting has been used for long and the use of AIC and BIC for the same has been discussed in Shi et al. (2002)[11].

3.2.1 Akaike Information Criterion

The Akaike Information Criteria(AIC) uses Kullback-Leibler information (KLI) as a tool for model selection. The K-L information I, for two models f and g is defined as:

$$I(f, g) = \int f(x) log \left(\frac{f(x)}{g(x|\theta)} \right) dx \tag{3.6}$$

for continuous functions denotes the information lost when $g(x|\theta)$ is used as an approximate model for the reality f, or is the distance from g to f. Similarly for discrete distributions the K-L information or the K-L distance is defined as

$$I(f, g) = \sum_{i=1}^{k} p_i . log \left(\frac{p_i}{\pi_i} \right) \tag{3.7}$$

where k is the total possible number of outcomes, p_i is the true possibility of the ith outcome and π_i is the model probability of the i th outcome. The K-L information $I(f, g)$ is always positive and $T(f, g) = 0$ only when $f = g$ as the approximate model is exactly equal to the true model then the distance between the two is zero. Thus

this tool can be used to find out the relative distance of different models from the true model as an approximate model becomes closer to reality by minimising $I(f,g)$. To compute $I(f,g)$, however, both f and g must be known. But to find the relative distance between two models, this is not necessary. One can thus, find the relative accuracy amongst different models without knowing the how consistent these models are with reality. From eq. 3.6,

$$I(f,g) = \int f(x)log(f(x))dx - \int f(x)log(g(x|\theta))dx \tag{3.8}$$

$$I(f,g) = E_f[log(f(x))] - E_f[log(g(x|\theta))] \tag{3.9}$$

where E_f is the expectation of $f(x)$ and $E_f[log(f(x))]$ is a constant depending only upon the true model and is an unknown. Hence, eq. 3.9 can be written as

$$I(f,g) - C = -E_f[log(g(x|\theta))] \tag{3.10}$$

where, $I(f,g) - C$ is the relative distance between f and g. For different approximate models, this can be written as

$$I(f,g_i) - C = -E_f[log(g(x|\theta_i))] \tag{3.11}$$

and g_i is the better fitting model if $I(f,g_i)$ is the smallest relative distance. Moreover, $I(f,g_1) - I(f,g_2) = E_f[log(g(x|\theta_2))] - E_f[log(g(x|\theta_1))]$ can be computed without the knowledge of the real model.

There must exist a value of θ or a model $g(x|\theta)$ for which the K-L distance is minimised, i.e, there exists a model which is closest to the real model and such a value for θ from the assumed models can be estimated using Maximum Likelihood analysis. Thus, $g(x|\theta_o)$ is the closest given approximate model to $f(x)$, the real model.

In data analysis, however, such parameters are estimated with a substantial amount of uncertainty and the approximate models are based on the estimation of these parameters $\hat{\theta_o}$ rather than their real values θ_o. Thus model selection deals with minimising the expected K-L distance over the known K-L distance. In Akaike(1973)[12], it has been shown that the maximum log-likelihood is biased due to the number of parameters in a model and can be corrected by:

$$2log(\mathcal{L}(\hat{\theta}|data)) - 2K = C - \hat{E}[I(f,\hat{g})] \tag{3.12}$$

where the bias correction K is the number of parameters in an approximate model.So,

$$AIC = -2log(\mathcal{L}(\hat{\theta}|data)) + 2K \tag{3.13}$$

which is an estimate of the expected relative K-L distance between two approximate models fitted to an unknown real model. In the case of least squares regression statistics, AIC can be computed as

$$AIC = nlog(\hat{\sigma}^2) + 2K \tag{3.14}$$

where $\hat{\sigma}^2$ is the sum of the estimated residuals in an approximate model and for chi square statistics

$$AIC = \chi^2 + 2K \tag{3.15}$$

and the likelihood of the model is given by

$$\mathcal{L}_\alpha = \frac{exp(-AIC_\alpha/2)}{exp(-AIC_1/2) + exp(-AIC_2/2)} \tag{3.16}$$

3.2.2 Bayesian Information Criterion

The Bayesian Information Criterion (BIC) involves an equal prior probability to all approximate models g_i as π_i. The marginal likelihood or the likelihood of a model g_i, given the true model and the prior probabilities on θ_i is given by:

$$g_i(x, \pi_i) = \int g_i(x|\theta_i)\pi_i(\theta_i)d\theta_i \tag{3.17}$$

The marginal probability of the data can thus be written as

$$\int \left[\prod_{i=1}^{n} g(x_i|\theta)\right] \pi(\theta)d\theta \tag{3.18}$$

which can be written as

$$\int [\mathcal{L}(\theta|x, g)]\pi(\theta)d\theta \tag{3.19}$$

As data is generated, true values for θ is not obtained but an estimate $\hat{\theta}$ is obtained, so the marginal likelihood of the data can be written as:

$$\mathcal{L}(\theta|x, g) = \mathcal{L}(\hat{\theta}|x, g)e^{\frac{1}{2}(\theta-\hat{\theta})'V(\hat{\theta})^{-1}(\theta-\hat{\theta})} \tag{3.20}$$

where $V(\hat{\theta})$ is the $K \times K$ dimensional variance-covariance matrix of the maximum likelihood estimate(MLE). Thus, the marginal probability can now be written as:

$$\mathcal{L}(\hat{\theta}|x,g) \int e^{\frac{1}{2}(\theta-\hat{\theta})'V(\hat{\theta})^{-1}(\theta-\hat{\theta})}\pi(\theta)d\theta \tag{3.21}$$

This marginal probability becomes exact as n tends to infinity and the likelihood reaches $\hat{\theta}$ which converges to θ_o, the true model. As the prior probability π is uniform for all approximate models, it can be assumed as a constant and taken out of the integral. The normalised marginal probability can be written approximately as:

$$\mathcal{L}(\theta|\hat{x},g) \left[(2\pi)^{K/2}n^{-K/2}||V(\hat{\theta})^{-1}||^{1/2}\right] \tag{3.22}$$

Multiplying $-2 \times log$ and dropping the negligible terms, we get the BIC as :

$$-2log(\mathcal{L}(\hat{\theta}|x,g)) + Klog(n) \tag{3.23}$$

For data using chi square statistics, the BIC is defined as:

$$BIC = \chi^2 + log(n)K \tag{3.24}$$

1

[1]For a detailed discussion, refer Model Selection and Multimodel Inference:A Practical Information- Theoretic Approach, Second Edition[8]

Chapter 4

Cosmological Tests using Angular Diameter Distance

Hoyle in 1959 proposed the use of cosmological objects or structures with no evolutionary effects to measure cosmic distances termed as standard rulers. Supernovae type Ia were considered standard candles as they gave fairly constant luminosity and the observed 40% scatter in the peak luminosity was corrected using Phillip's relation to obtain their luminosity distance and hence used to constrain the cosmological parameters. This use of Supernova Ia as standard candles is however not completely justified and any systematic differences between high redshift and low redshift type Ia supernova is still a controversial subject. Simultaneously in the late 20th century a search for standard rulers to constrain cosmological parameters was going on. Radio galaxies of kpc scale, were first considered as metric rulers but their angular sizes' relation with redshift was an uncertain indicator of an actual evolution in size or a relation arising due to selection effects (Wei et al(2015)[9]). With a larger sample over a range of redshift facilitated by the Very Large Baseline Interferometer(VLBI), it was demonstrated that the angular size-redshift relation was consistent with the FLRW model(Gurvits et al. 1999)[13]. However, this does not seem consistent with an expanding cosmology, unless the selected radio galaxies' sizes have increased six times from redshift 3.2 to now (McIntosh et al. 2005)[14]. Galaxy clusters as demonstrated in earlier sections, can be used as standard rulers. The combined data from SZE and X-ray emission combined, provides a method to measure their angular di-

ameter distances which can be compared to the angular diameter distance derived for different cosmologies theoretically and constrain the cosmological parameters.
In this chapter, we first consider a larger dataset compiled by Bonamente et al.(2006)[15] and perform parameter fitting to find the better fitting cosmological model and parameters. Then we calculate the angular diameter distance and perform parameter fitting for data compiled in Reese et al. (2002)[16], taking into account cluster morphology to understand the effects of morphology on parameter estimation and discuss the results.

4.1 The Cluster Angular Size Sample

We use the calculated angular diameter distances to 38 galaxy clusters of redshift range $0.142 \leq z \leq 0.89$ which uses X-ray Chandra data and SZE data from Owens Valley Radio Observatory (OVRO) and Berkely-Illinois-Maryland Association (BIMA) array, given in Wei et al. (2014)[9].

Table 4.1: Angular Diameter Distance of Galaxy Clusters using data from X-ray Chandra and BIMA-OVRO arrays

Cluster	z	$D_a(Mpc)$
Abell 1413	0.142	780^{+180}_{-130}
Abell 2204	0.152	610^{+60}_{-70}
Abell 2259	0.164	580^{+290}_{-250}
Abell 586	0.171	520^{+150}_{-120}
Abell 1914	0.171	440^{+40}_{-50}
Abell 2218	0.176	660^{+140}_{-110}
Abell 665	0.182	660^{+90}_{-100}
Abell 1689	0.183	650^{+90}_{-90}
Abell 2163	0.202	520^{+40}_{-50}
Abell 773	0.217	980^{+170}_{-140}

Table 4.2: Angular Diameter Distance of Galaxy Clusters using data from X-ray Chandra and BIMA-OVRO arrays

Cluster	z	$D_a(Mpc)$
Abell 2261	0.224	730^{+200}_{-130}
Abell 2111	0.229	640^{+200}_{-170}
Abell 267	0.23	600^{+110}_{-90}
RX J2129.7+0005	0.235	460^{+110}_{-80}
Abell 1835	0.252	1070^{+20}_{-80}
Abell 68	0.255	630^{+160}_{-190}
Abell 697	0.282	880^{+300}_{-230}
Abell 611	0.288	780^{+180}_{-180}
ZW 3146	0.291	830^{+20}_{-20}
Abell 1995	0.322	1190^{+150}_{-140}
MS 1358.4+6245	0.327	1130^{+90}_{-100}
Abell 370	0.375	1080^{+190}_{-200}
MACS J2228.5+2036	0.412	1220^{+240}_{-230}
RX J1347.5-1145	0.451	960^{+60}_{-80}
MACS J22149.9-1359	0.483	1440^{+270}_{-230}
MACS J1311.0-0310	0.49	1380^{+470}_{-370}
CL 0016+1609	0.541	1380^{+220}_{-220}
MACS J1149.5+2223	0.544	800^{+190}_{-160}
MACS J1423.8+2404	0.545	1490^{+60}_{-30}
MS 0451.6-0305	0.55	1420^{+260}_{-230}
MACS J2129.4-0741	0.57	1330^{+370}_{-280}
MS 2053.7-0449	0.583	2480^{+410}_{-440}
MACS J0647.7+7015	0.584	770^{+210}_{-180}
MACS J0744.8+3927	0.686	1680^{+480}_{-380}
MS1137.5+6625	0.784	2850^{+520}_{-630}
RX J1716.4+6708	0.813	1040^{+510}_{-430}
MS 1054.5-0.321	0.826	1330^{+280}_{-260}
CL J1226.9+3332	0.89	1080^{+420}_{-280}

4.1.1 Parameter fits and Results

We have considered three different models for fitting the hubble constant H_o:

1. Concordance model(ΛCMD): The standard model of cosmology for flat universe with the matter density parameter $\Omega_m = 0.3$ and the equation of state parameter for dark energy $w_{de} = -1$ in the Friedmann Model.

2. Einstein- deSitter Model: Matter only flat universe with the matter density parameter $\Omega_m = 1.0$.

3. $R_H = ct$ model: Friedmann model which takes the dark energy equation of state parameter $w = -1/3$ at all times in the history of the universe.

The Hubble constant H_o is optimised by minimising the χ^2 function, i.e,

$$\chi^2 = \sum_{i=1}^{38} \frac{D_a^{the}(z_i) - D_a^{obs}(z_i)}{\sigma_{tot}^2} \tag{4.1}$$

Where σ_{tot}^2 includes the systematic, statistical and modelling errors which have been referred from Bonamante et al.(2006).

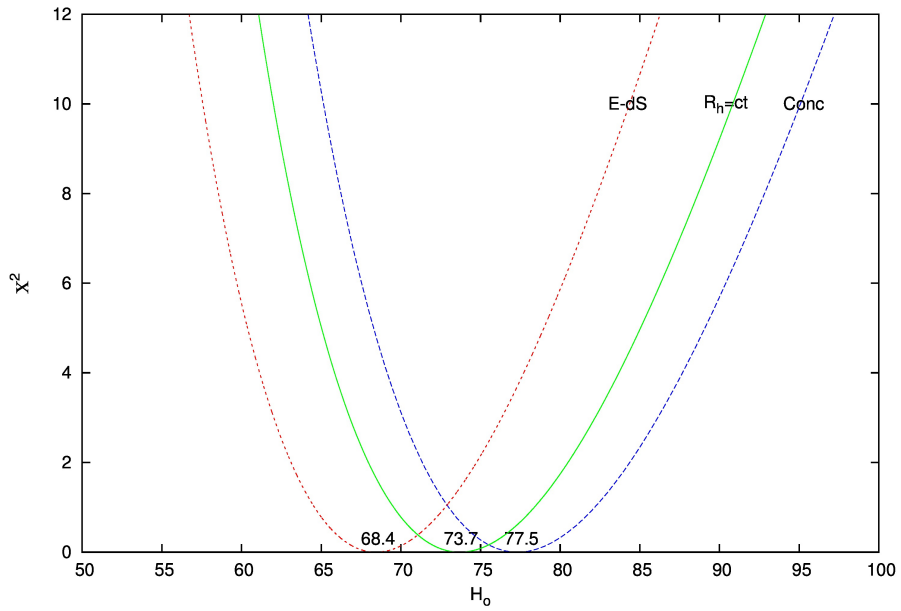

Figure 4.1: Reduced χ^2 function constraining H_o for sample from X-ray Chandra and BIMA-OVRO for $R_H = ct$ universe, concordance and Einstein-deSitter models of universe

From the χ^2 statistics, the optimised H_o was obtained as $73.7^{+19.82}_{-12.89} Kms^{-1}Mpc^{-1}$ for $R_H = ct$ model, $77.5^{+15.99}_{-16.675} Kms^{-1}Mpc^{-1}$ for ΛCDM concordance model and $68.44^{+19.91}_{-12.59} Kms^{-1}Mpc^{-1}$ for Einstein deSitter model of the universe. Fig(4.1) shows the reduced χ^2 functions for optimising the Hubble constant.

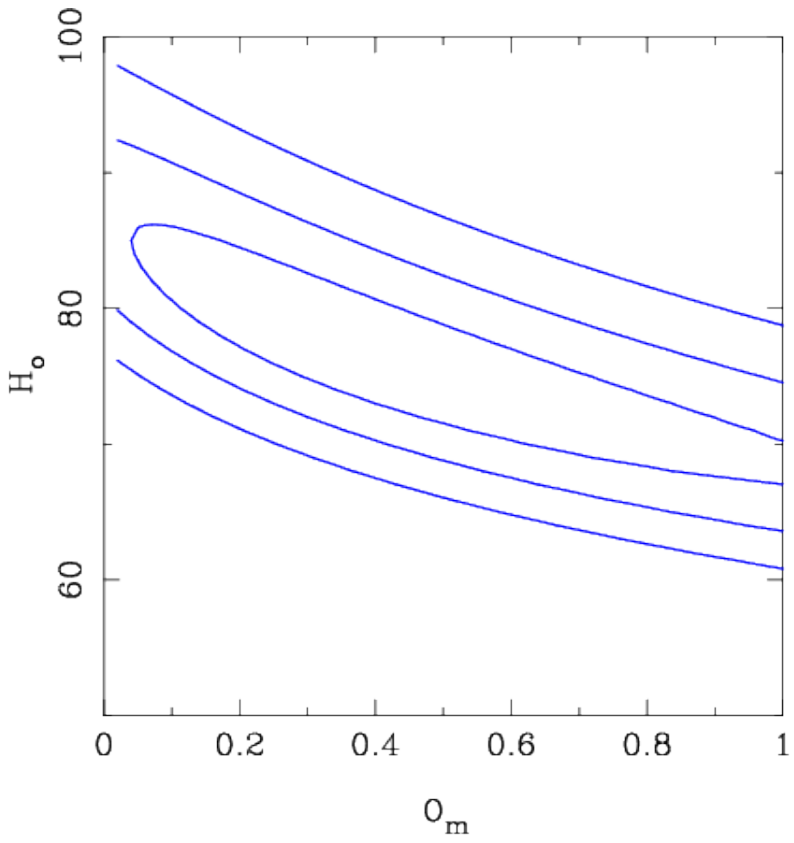

Figure 4.2: Constant χ contours for relaxed parameters in ΛCDM model

For ΛCDM model of cosmology, the equation of state parameter for dark energy is $w_{de} = -1$. Relaxing the matter density parameter and the Hubble constant and performing chi-square analysis of the same give the best fit parameter as $\Omega_m = 0.37$ and $H_o = 76.0 Kms^{-1}Mpc^{-1}$.The χ^2 per degree of freedom for optimised Hubble parameter for this model of the universe with constant Ω_m(Concordance model) = $\chi^2_{dof} = 0.52$ and for parameters allowed to vary $\chi^2_{dof} = 0.55$. Fig(4.2) shows $1\sigma, 2\sigma$ and 3σ constant χ contours for relaxed parameters in ΛCDM universe.

For $wCDM$ model of cosmology, where the equation of state parameter of dark energy is constant but, $w_{de} \neq -1$ and Ω_m and H_o are variables. In this analysis, we

have considered the value for the matter density as$\Omega_m = 0.3$ and kept w_{de} and H_o as variables. By performing the χ^2 analysis of the same we get $w_{de} = -0.90$ and $H_o = 76.0 Kms^{-1}Mpc^{-1}$ as the best-fit parameters and the $\chi^2_{dof} = 0.54$. Fig(4.3) shows $1\sigma, 2\sigma$ and 3σ constant χ contours for relaxed parameters in wCDM universe.Fig(4.3) shows $1\sigma, 2\sigma$ and 3σ constant χ contours for relaxed parameters in $wCDM$ universe.

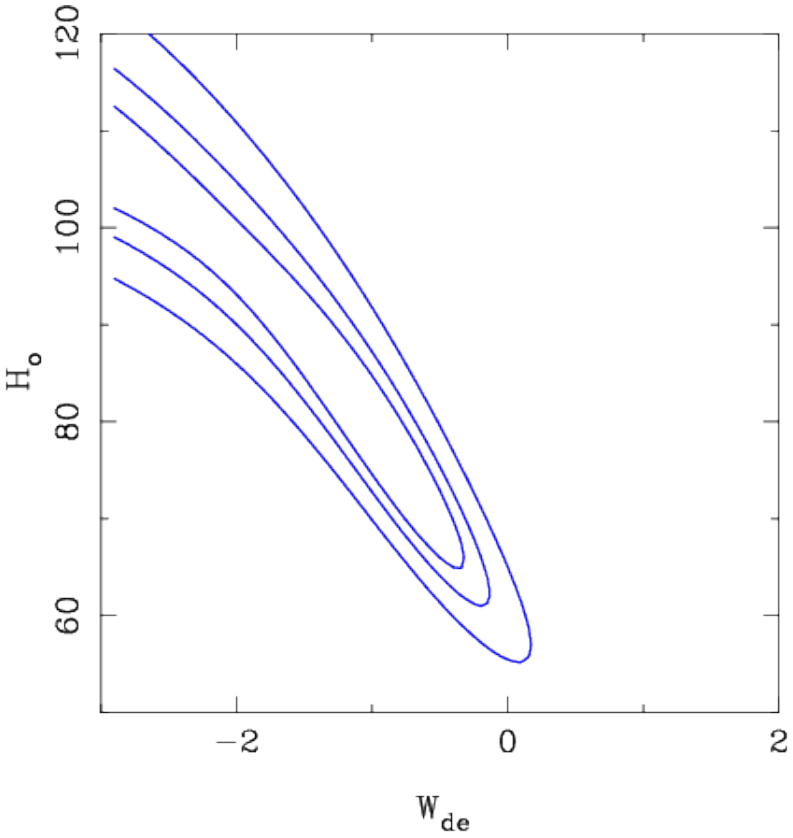

Figure 4.3: Constant χ contours for relaxed parameters in $wCDM$ model

The $R_H = ct$ model of cosmology only deals with one free parameter, the Hubble constant. Fig(4.4) shows the data points for ADD for 38 galaxy clusters and theoretical fits for $R_H = ct$ model with $H_o = 73.7^{+19.82}_{-12.89} Kms^{-1}Mpc^{-1}$, along with the theoretical fit for ΛCDM model using the best-fit parameters obtained. The χ^2 per degree of freedom is $\chi^2_{dof} = 0.54$.

From fig(4.4), the ΛCDM and $R_H = ct$ models of cosmology appear to fit the data comparably well, however since the models derive different best-fit parameters for the observed data and the number of free parameters are different for the two models,

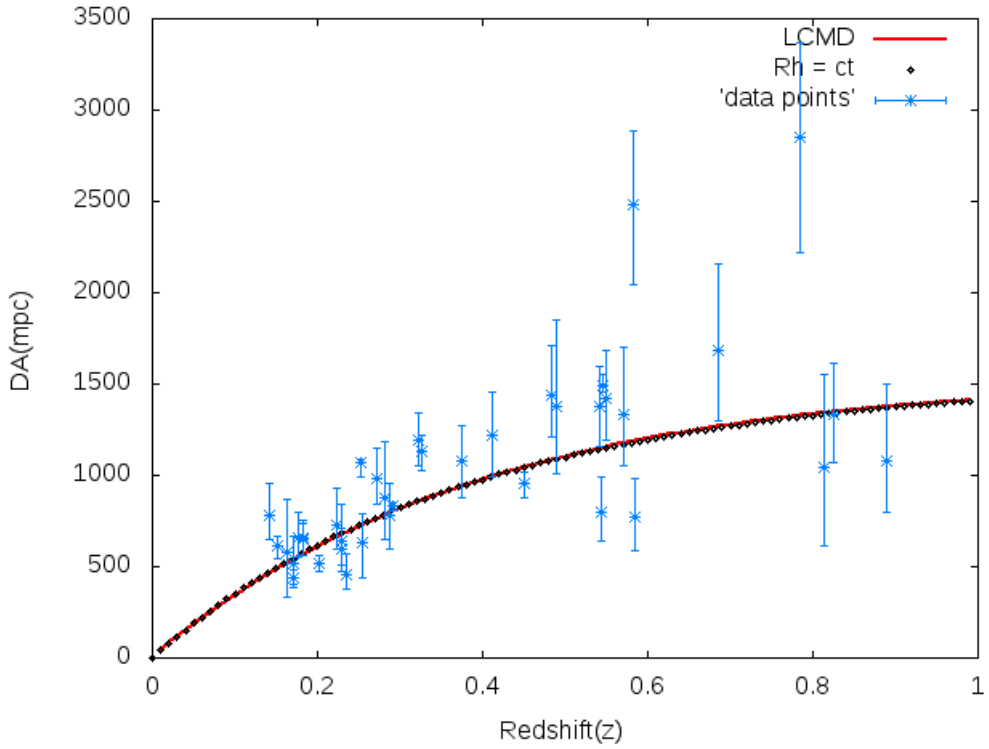

Figure 4.4: Angular Diameter Distances for 38 galaxy clusters with error bars and the best fit theoretical curves for ADD as a function of redshift (z) for ΛCDM universe and the $R_H = ct$ model of cosmology

likelihood analysis is needed to select a model of cosmology as the more probable model of the universe.

We use AIC and BIC (chapter 3) along with likelihood estimates for model selection. From eq.(3.11)

$$AIC = \chi^2 + 2K$$

For two models that have been separately fitted, the one with the least AIC is deemed to be more likely with the likelihood described as

$$\mathcal{L}_\alpha = \frac{exp(-AIC_\alpha/2)}{exp(-AIC_1/2) + exp(-AIC_2/2)}$$

From eq.(3.20) Bayesian information criterion is defined as

$$BIC = \chi^2 + ln(n)K$$

From the obtained parameters for different models AIC analysis prefers $R_H = ct$ universe over the ΛCDM model and $wCDM$ model by $\approx 70.32\%$ over $\approx 29.67\%$ on

ΛCDM and $\approx 70.41\%$ over $\approx 29.58\%$ on $wCDM$. BIC also prefers the $R_H = ct$ universe over the ΛCDM model and $wCDM$ model by $\approx 83.96\%$ over $\approx 16.03\%$ on ΛCDM and $\approx 84.36\%$ over $\approx 15.63\%$ on $wCDM$.

4.2 Effects of Morphology on Angular Diameter Distance: Circular and Elliptical β-Models

The projection of galaxy clusters are rarely circular, but the analysis of X-ray imaging data and SZE data assumes a spherical symmetry. By correcting for this bias, by modelling the X-ray surface brightness and β using elliptical β-model, it is observed that there is no significant change in the surface brightness, but there is a change in the core radii which effects the θ_c(de Fillipis et al.2005)[17]. The projection on the plane of sky for the galaxy clusters for modelled with elliptical β-model is given by the relation:

$$\theta_c|_{ell} = \theta_c \frac{2e_{proj}}{1 + e_{proj}} \tag{4.2}$$

Thus the angular diameter distance for clusters modelled with elliptical β- model is given by the relation:

$$D_a|_{ell} = D_a \frac{1 + e_{proj}}{2e_{proj}} \tag{4.3}$$

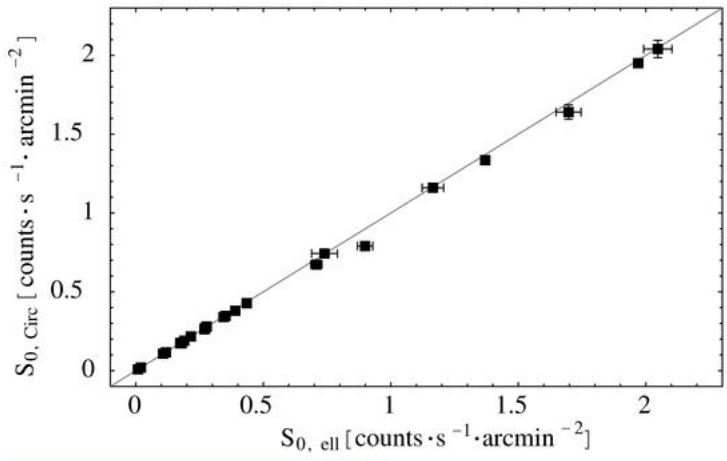

(a)

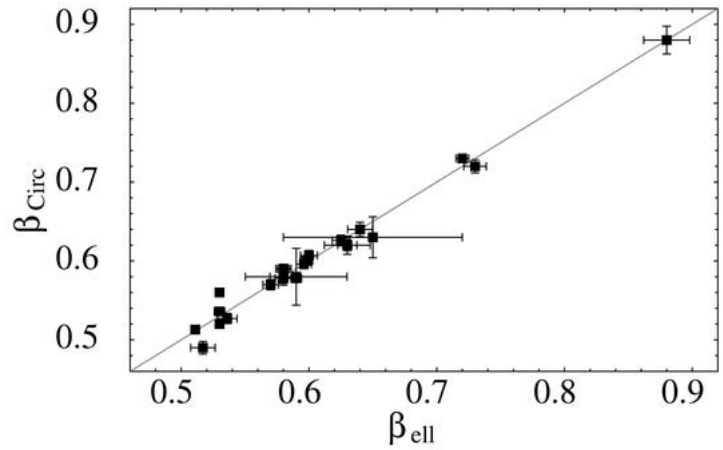

(b)

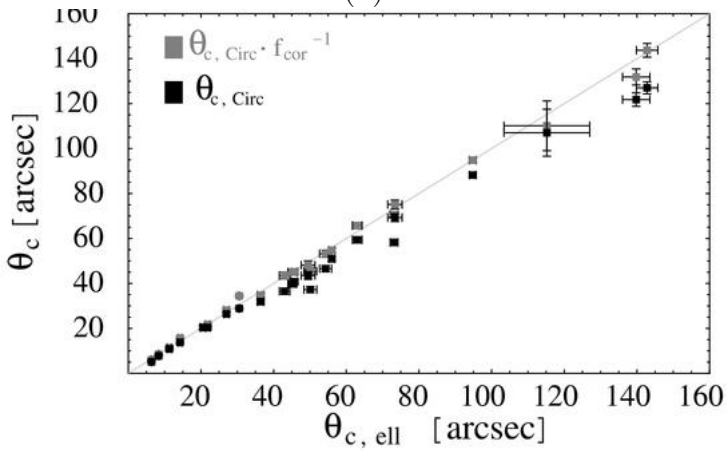

(c)

Figure 4.5: Comparison of quantities for galaxy clusters modelled with circular β-model and elliptical β-model. (a) shows the variation of the surface brightness, (b) shows the variation in the slopeβ and (c) shows the variation in the core radii of the cluster.(de Fillipis et al 2005)[17]

4.2.1 Galaxy Cluster Sample

The distance calculations require SZE, X-ray imaging and spectroscopic data sets for galaxy clusters. For the SZE data Owens Valley Radio Observatory(OVRO) and Berkely-Illinois-Maryland Association interferometers(BIMA) have been used to observe X-ray clusters with redshift greater than 0.14 and declination greater than $-15\,\mathrm{deg}$ for $0.1 - 2.4keV$ band for ROSAT clusters. Table 4.3. contains the compiled

positions, redshifts and X-ray luminosities.

Table 4.3: Cluster Sample

Cluster	R.A. (J2000)	Decl.(J2000)	redshift	L_x $(\times 10^{44} h^{-2} ergs s^{-1})$
MS 1137.5+6625	...	...	0.784	5.4
MS 0451.6-0305.....	04 54 22.1	-03 01 25	0.550	20.0
Cl 0016+16	00 18 31.	16 20 45	0.546	14.6
RX J1347.5-1145	13 47 30.7	-11 45 09	0.451	73.0
A370	02 39 55.5	-01 34 06	0.374	11.7
MS 1358.4+6245	13 59 50.6	62 31 05	0.327	10.6
A1995	14 53 00.5	58 03 19	0.322	13.4
A611	...	...	0.288	8.6
A697	...	...	0.282	19.2
A1835	14 01 02.0	02 52 42	0.252	32.6
	14 01 00.5	02 51 53		
A2261	17 22 17.1	32 09 14	0.224	20.6
A773	...	...	0.216	12.1
A2163	16 15 43.3	-06 08 40	0.202	37.5
	04 54 01.1	02 57 47		
A520	04 54 17.0	02 55 32	0.202	14.5
	04 54 20.3	02 54 56		
A1689	13 11 31.6	-01 19 33	0.183	20.7
	13 11 30.1	-01 20 37		
A665	08 31 30.9	65 52 35	0.182	15.7
	16 35 22.1	66 13 23		
A2218	16 35 47.7	66 14 46	0.171	8.2
	16 36 16.0	66 14 23		
A1413	11 55 08.7	23 26 17	0.142	10.9

Table 4.4 contains ROSAT X-ray data, Gas temperature and the cooling functions (calculated using the Raymond-Smith spectrum(1977)[18] with relativistic corrections (Reese et al. 2000)[19].

Table 4.4: ROSAT X-ray data and Cooling Functions

Cluster	kT_e (keV)	Λ_{eH} ($\times 10^{-24} ergss^{-1}cm^3$)
MS 1137.5+6625	$5.7^{+1.3}_{-0.7}$	7.751
MS 0451.6-0305.....	$10.4^{+1.0}_{-0.8}$	6.948
Cl 0016+16	$7.55^{+0.72}_{-0.58}$	6.922
RX J1347.5-1145	$9.3^{+0.7}_{-0.6}$	6.922
A370	$6.6^{+0.7}_{-0.5}$	6.790
MS 1358.4+6245	$7.48^{+0.5}_{-0.42}$	6.717
A1995	$8.59^{+0.86}_{-0.67}$	6.434
A611	$6.6^{+0.6}_{-0.6}$	6.511
A697	$9.8^{+0.7}_{-0.7}$	6.334
A1835	$8.21^{+0.19}_{-0.17}$	6.462
A2261	$8.82^{+0.37}_{-0.32}$	6.359
A773	$9.29^{+0.41}_{-0.36}$	6.171
A2163	$12.2^{+1.1}_{-0.7}$	6.135
A520	$8.33^{+0.46}_{-0.4}$	6.119
A1689	$9.66^{+0.22}_{-0.2}$	6.158
A665	$9.03^{+0.35}_{-0.31}$	6.102
A2218	$7.05^{+0.22}_{-0.21}$	6.112
A1413	$7054^{+0.17}_{-0.16}$	6.133

Table 4.5 contains the modelled ICM parameters, β, θ_c, surface brightness and SZE temperature decrement.

Table 4.5: ICM Parameters

Cluster	β	θ_c (arcsec)	e_{proj}	$S_x \times 10^{-12}$ $\left(ergss^{-1}cm^{-2}arcmin^{-2}\right)$	ΔT (μK)
MS 1137.5+6625	$0.786^{+0.220}_{-0.120}$	$19.4^{+6.4}_{-4.0}$	1.113 ± 0.014	$0.443^{+0.074}_{-0.059}$	-818^{+98}_{-0113}
MS 0451.6-0305.....	$0.806^{+0.052}_{-0.043}$	$34.7^{+3.9}_{-3.5}$	1.307 ± 0.015	$0.956^{+0.086}_{-0.022}$	-1431^{+98}_{-93}
Cl 0016+16	$0.749^{+0.024}_{-0.018}$	$42.3^{+2.4}_{-2.0}$	1.205 ± 0.013	$0.617^{+0.022}_{-0.028}$	-1242^{+105}_{-105}
RX J1347.5-1145	$0.604^{+0.011}_{-0.012}$	$9.0^{+0.5}_{-0.5}$	1.453 ± 0.019	$27.4^{+1.6}_{-1.4}$	-3950^{+350}_{-350}
A370	$0.518^{+0.090}_{-0.080}$	$39.5^{+10.5}_{-10.5}$	1.564 ± 0.018	$0.270^{+0.043}_{-0.030}$	-1253^{+218}_{-533}
MS 1358.4+6245	$0.622^{+0.015}_{-0.015}$	$18.2^{+1.4}_{-1.5}$	1.325 ± 0.019	$1.70^{+0.15}_{-0.11}$	-784^{+90}_{-90}
A1995	$0.770^{+0.117}_{-0.063}$	$38.9^{+6.9}_{-4.3}$	1.242 ± 0.010	$1.08^{+0.08}_{-0.07}$	-1023^{+83}_{-77}
A611	$0.565^{+0.050}_{-0.040}$	$17.5^{+3.5}_{-3.5}$	1.14 ± 0.05	$2.01^{+0.36}_{-0.26}$	-853^{+120}_{-140}
A697	$0.540^{+0.045}_{-0.035}$	$37.8^{+5.6}_{-4.0}$	1.334 ± 0.016	$1.02^{+0.07}_{-0.08}$	-1410^{+160}_{-180}
A1835	$0.595^{+0.007}_{-0.005}$	$12.2^{+0.6}_{-0.5}$	1.225 ± 0.012	$20.2^{+1.4}_{-1.0}$	-2502^{+150}_{-175}
A2261	$0.516^{+0.014}_{-0.013}$	$15.7^{+1.2}_{-1.1}$	1.022 ± 0.017	$4.31^{+0.26}_{-0.26}$	-1697^{+220}_{-200}
A773	$0.597^{+0.064}_{-0.032}$	$45.0^{+7.0}_{-5.0}$	1.237 ± 0.022	$0.828^{+0.065}_{-0.065}$	-1260^{+160}_{-160}
A2163	$0.674^{+0.011}_{-0.008}$	$87.5^{+2.5}_{-2.0}$	1.206 ± 0.004	$1.36^{+0.03}_{-0.03}$	-1900^{+140}_{-140}
A520	$0.844^{+0.040}_{-0.040}$	$123.3^{+8.0}_{-8.0}$	1.06 ± 0.05	$0.408^{+0.018}_{-0.018}$	-662^{+95}_{-95}
A1689	$0.609^{+0.005}_{-0.005}$	$26.6^{+0.7}_{-0.7}$	1.141 ± 0.012	$6.01^{+0.18}_{-0.15}$	-1729^{+105}_{-120}
A665	$0.615^{+0.006}_{-0.006}$	$71.7^{+1.5}_{-1.5}$	1.238 ± 0.012	$0.678^{+0.012}_{-0.012}$	-728^{+150}_{-150}
A2218	$0.692^{+0.008}_{-0.008}$	$67.5^{+1.5}_{-1.8}$	1.162 ± 0.009	$0.708^{+0.016}_{-0.014}$	-731^{+125}_{-100}
A1413	$0.639^{+0.009}_{-0.009}$	$47.7^{+2.0}_{-2.0}$	1.473 ± 0.019	$2.04^{+0.09}_{-0.09}$	-856^{+110}_{-110}

Using eq(2.26) and eq(4.3) calculated angular diameter distance for both circular β model and elliptical β model is tabulated in table 4.6.

Table 4.6: Calculated Angular Diameter Distances

Cluster	$D_a\|_{cir}$ (Mpc)	$D_a\|_{ell}$ (Mpc)
MS 1137.5+6625	$2878.27^{+728.04}_{-137.19}$	$2732.16^{+703.08}_{-147.48}$
MS 0451.6-0305.....	$1124.43^{+159.67}_{-166.70}$	$992.37^{+145.11}_{-152.86}$
Cl 0016+16	$1832.28^{+104.32}_{-68.73}$	$1676.42^{+103.20}_{-71.49}$
RX J1347.5-1145	$1081.83^{+46.14}_{-8.94}$	$913.19^{+43.55}_{-12.52}$
A370	$3932.12^{+827.27}_{-2839.75}$	$3223.13^{+660.79}_{-2323.66}$
MS 1358.4+6245	$780.69^{+13.85}_{-24.64}$	$684.94^{+16.24}_{-17.46}$
A1995	$1084.13^{+65.63}_{-49.33}$	$978.51^{+62.51}_{-48.23}$
A611	$897.28^{+37.97}_{-25.19}$	$842.19^{+51.47}_{-6.09}$
A697	$881.01^{+90.09}_{-128.05}$	$770.71^{+74.49}_{-108.59}$
A1835	$904.87^{+14.11}_{-28.17}$	$821.77^{+16.34}_{-22.05}$
A2261	$934.04^{+96.20}_{-116.94}$	$923.98^{+86.92}_{-108.92}$
A773	$1284.90^{+222.65}_{-164.20}$	$1161.81^{+190.68}_{-140.27}$
A2163	$718.97^{+34.44}_{-9.39}$	$657.56^{+32.44}_{-7.61}$
A520	$644.37^{+81.24}_{-100.95}$	$626.13^{+63.53}_{-85.40}$
A1689	$609.02^{+22.67}_{-41.01}$	$571.39^{+18.39}_{-35.83}$
A665	$413.73^{+132.15}_{-129.53}$	$373.96^{+120.03}_{-115.95}$
A2218	$926.37^{+241.12}_{-174.57}$	$861.79^{+220.45}_{-159.87}$
A1413	$514.55^{+78.93}_{-82.70}$	$431.94^{+63.69}_{-67.51}$

4.2.2 Parameter fits and Results

For each model of universe, best fit parameters are obtained by minimising the χ^2 function for H_o Hubble's Constant, i.e, minimising eq.(4.1)

Fig 4.6 shows the χ^2 functions for optimising the Hubble constant for differnt models of universe. The best-fit for Hubble constant obatined for the three models of universe i.e, $R_H = ct$, Einstein de-Sitter and concordance model, for circular and elliptical β model are tablulated in table 4.7

Table 4.7: Optimised Hubble Constant for different models of universe

	E-dS	$R_H = ct$	Conc
Circular β model	62.53	66.34	70.0
Elliptical β model	69.5	73.78	78.0

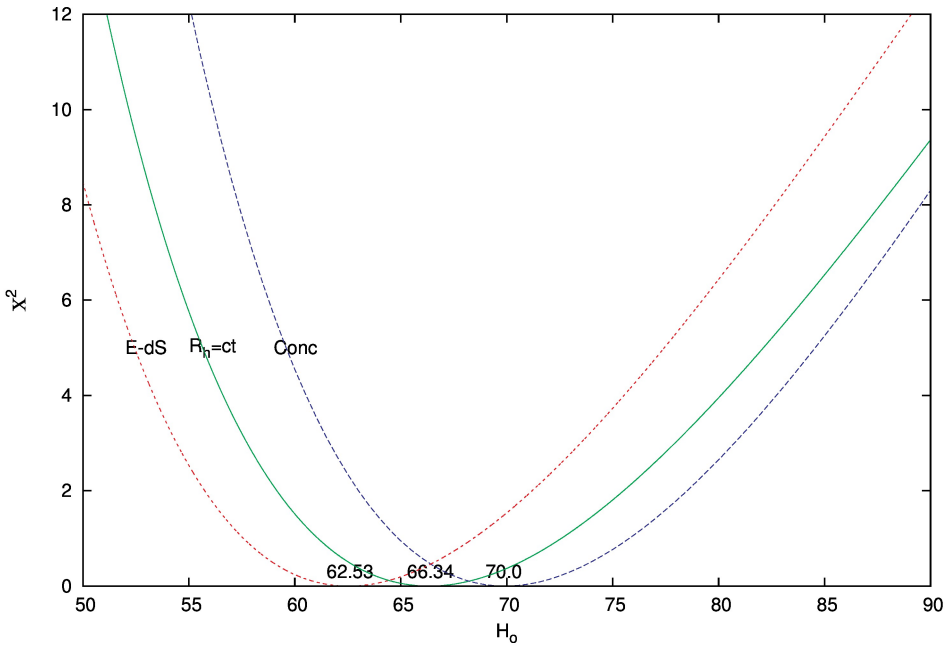

(a)

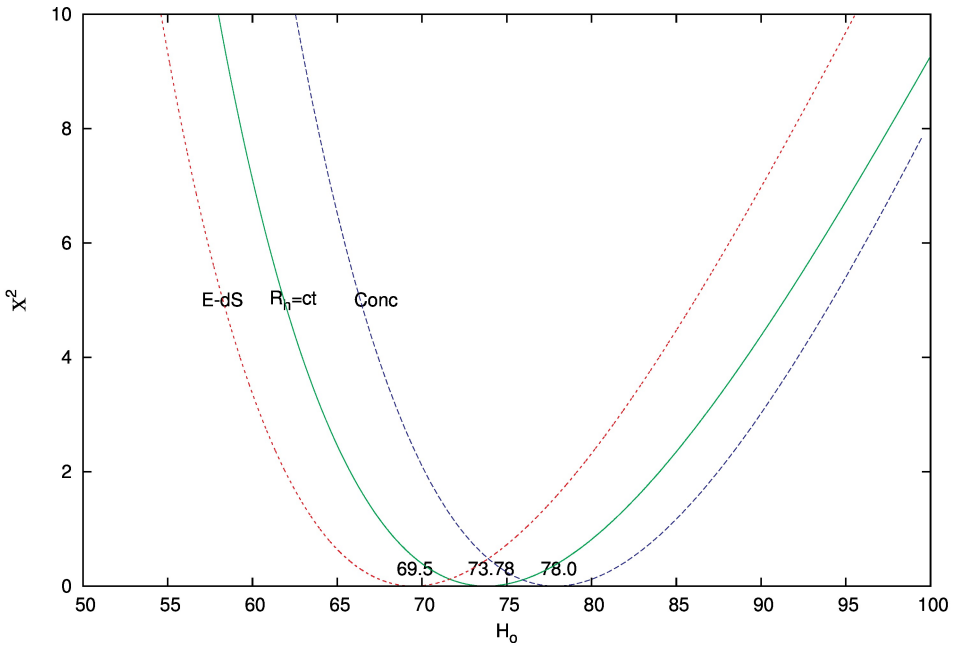

(b)

Figure 4.6: Constraining the Hubble parameter($kms^{-1}Mpc^{-1}$) for $R_H = ct$, Einstein de-Sitter universe and concordance universe for Galaxy cluster sample modelled with (a) circular β model and (b) elliptical β model

From χ^2 statistics, the optimised H_o for circularly modelled galaxy clusters were obtained as $62.53^{+20.22}_{-12.008} Kms^{-1}Mpc^{-1}$ for Einstein deSitter model, $66.34^{+20.015}_{-12.485} Kms^{-1}Mpc^{-1}$ for $R_H = ct$ model and $70.0^{+19.5}_{-12.5} Kms^{-1}Mpc^{-1}$ for ΛCDM concordance model. The χ^2_{dof}, the χ^2 per degree of freedom for these were calculated to be $0.537, 0.513$ and 0.31 respectively.From the χ^2 statistics analysis, the optimised values for H_o for elliptically modelled galaxy clusters were obtained as $69.495^{+19.85}_{-12.63} Kms^{-1}Mpc^{-1}$ for Einstein deSitter model, $73.78^{+19.67}_{-12.82} Kms^{-1}Mpc^{-1}$ for $R_H = ct$ model and $78.0^{+19.0}_{-13.0} Kms^{-1}Mpc^{-1}$ for ΛCDM concordance model. The χ^2_{dof}, the χ^2 per degree of freedom for these were calculated to be $0.781, 0.755$ and 0.630 respectively.

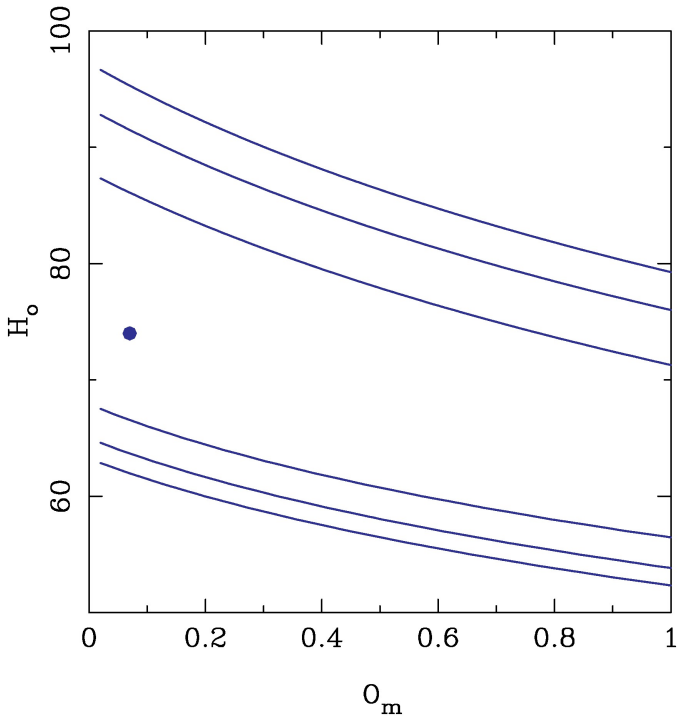

(a)

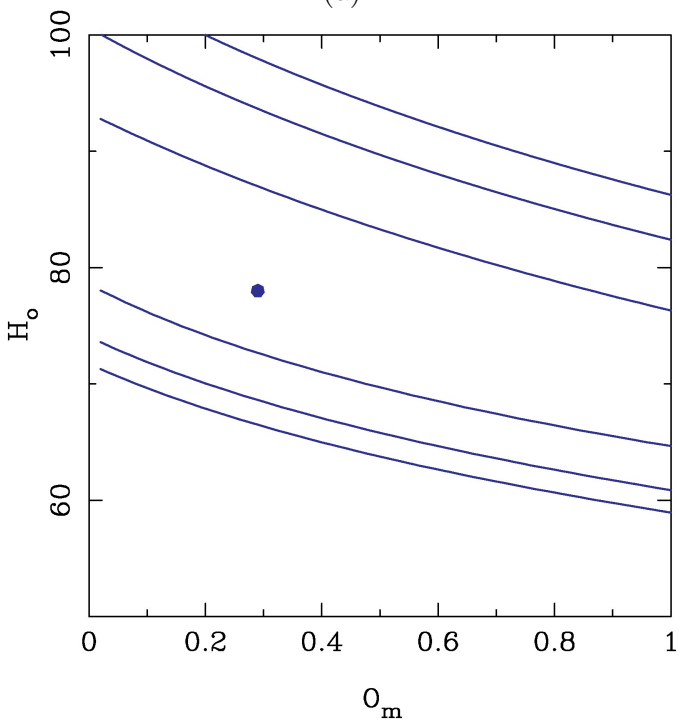

(b)

Figure 4.7: Constraining contours for Hubble parameter($kms^{-1}Mpc^{-1}$) and $\Omega_m$for flat ΛCDM model of the universe for Galaxy cluster sample modelled with (a) circular β model and (b) elliptical β model

For ΛCDM model($w_{de} = -1$), with relaxed parameters Ω_m and H_o, χ^2 analysis gave the best-fit parameters as 0.07 and 74.0 respectively for circularly modelled galaxy clusters and 0.29 and 78.0 respectively for elliptically modelled galaxy clusters. The χ^2 per degree of freedom was calculated as 0.57 and 1.046 for circularly and elliptically modelled galaxy clusters respectively.

For $wCDM$ model($\Omega_m = 0.3$), with relaxed parameters w_{de} and H_o, χ^2 analysis gave the best-fit parameters as -1.15 and 73.0 respectively for circularly modelled galaxy clusters and -0.9 and 77.0 respectively for elliptically modelled galaxy clusters. The χ^2 per degree of freedom was calculated as 0.89 and 1.045 for circularly and elliptically modelled galaxy clusters respectively.

Figure 4.8: Constraining contours for Hubble parameter($kms^{-1}Mpc^{-1}$) and $w_{de}$for flat $wCDM$ model of the universe for Galaxy cluster sample modelled with (a) circular β model and (b) elliptical β model

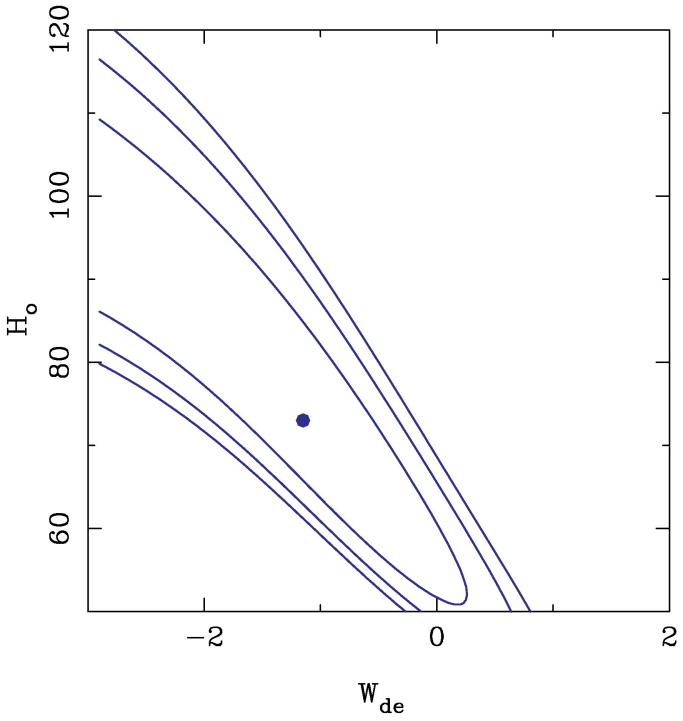

(a)

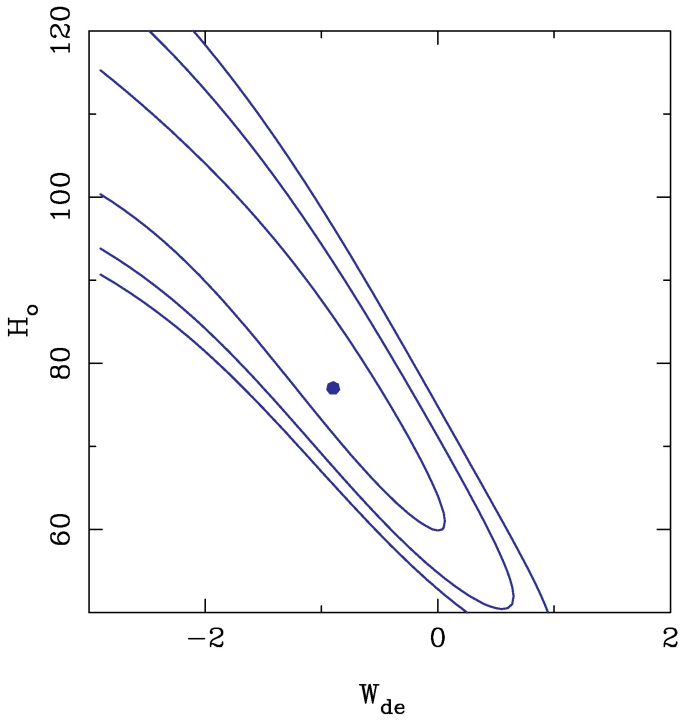

(b)

Fig.(4.9) shows the theoretical best-fit curves for angular diameter distance as a function of redshift for ΛCDM and $R_H = ct$ models of the universe along with the data points for galaxy clusters modelled with circular β model and elliptcial β model. The theoretical fits for the two different models are consistent with each other and with the data points, hence, preferred model can be found using likelihood analysis for the two models.

The likelihood analysis based on χ^2_{dof} and AIC prefers $R_H = ct$ model over ΛCDM and $wCDM$ models by $\approx 53.8\%$ over $\approx 15.21\%$ and $\approx 15.32\%$ respectively. Similarly, likelihood analysis using BIC weights prefer $R_H = ct$ model over ΛCDM by $\approx 84.4\%$ and $wCDM$ models by $\approx 85.15\%$ for circularly modelled galaxy clusters. For elliptically modelled galaxy clusters, he likelihood analysis based on χ^2_{dof} and AIC prefers $R_H = ct$ model over ΛCDM and $wCDM$ models by $\approx 78.1\%$ over $\approx 10.9\%$ and $\approx 10.9\%$ respectively. Similarly, likelihood analysis using BIC weights prefer $R_H = ct$ model over ΛCDM by $\approx 95.03\%$ and $wCDM$ models by $\approx 95.02\%$.

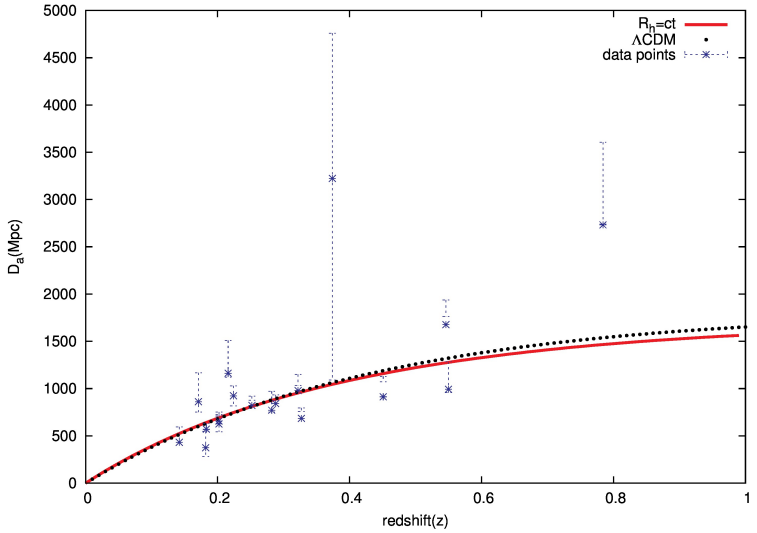

(a)

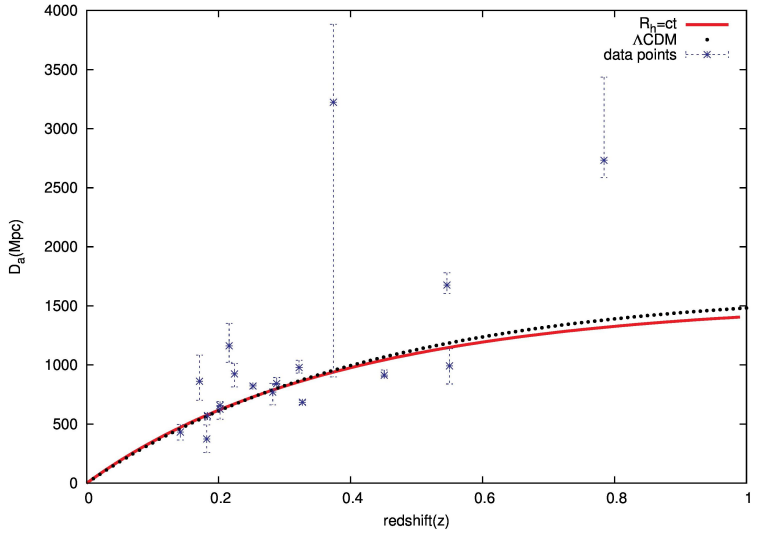

(b)

Figure 4.9: Angular Diameter Distances for 38 galaxy clusters with error bars and the best-fit theoretical curves for ADD as a function of redshift (z) for ΛCDM universe and the $R_H = ct$ model of cosmology for (a) circularly modelled galaxy clusters (b) elliptically modelled galaxy clusters.

4.3 Summary and Conclusions

In this work we have investigated the constraints on cosmological parameters using angular diameter distance for two data sets:

Data Sample 1: Data for 38 galaxy clusters from X-Ray Chandra and BIMA-OVRO arrays

Data Sample 2.a: Data for 18 galaxy clusters from ROSAT and BIMA-OVRO arrays modelled using Circular-β model

Data Sample 2.b: Data for 18 galaxy clusters from ROSAT and BIMA-OVRO arrays modelled using Elliptical-β model

Table 4.8: Best-Fit Parameters and χ^2_{dof} Obtained

	Sample data 1	Sample data 2.a	Sample data 2.b
$R_H = ct$	$H_o = 73.7$	$H_o = 66.34$	$H_o = 73.78$
	$\chi^2_{dof} = 0.54$	$\chi^2_{dof} = 0.513$	$\chi^2_{dof} = 0.755$
	$\Omega_m = 0.37$	$\Omega_m = 0.07$	$\Omega_m = 0.29$
ΛCDM	$H_o = 76.0$	$H_o = 74.0$	$H_o = 78.0$
	$\chi^2_{dof} = 0.55$	$\chi^2_{dof} = 0.57$	$\chi^2_{dof} = 1.046$
	$w_{de} = -0.90$	$w_{de} = -1.15$	$w_{de} = -0.9$
$wCDM$	$H_o, = 76.0$	$H_o = 73.0$	$H_o = 77.0$
	$\chi^2_{dof} = 0.54$	$\chi^2_{dof} = 0.89$	$\chi^2_{dof} = 1.045$

Comparing these results to the best fit parameters obtained from Supertnovae Type Ia data :$0.05 \leq \Omega_m \leq 0.43$ and $-1.57 \leq w_{de} \leq -0.66$ with best fit parameters $\Omega_m = 0.29$ and $w_{de} = -1.09$ [20] and $69.4 \leq H_o \leq 79.94$ with best-fit at $H_o = 74 Kms^{-1}Mpc^{-1}$[21], we can see that all the parameters calculated are within the confidence interval fron Supernovae Type Ia data. Sample 1 and Sample 2.b slighly over determines the best-fit for Hubble parameter for ΛCDM and $wCDM$ models. Sample 2.a underdetermines Ω_m and w_{de} for ΛCDM and $wCDM$ models and H_o for $R_H = ct$ model. And from observations, $R_H = ct$ universe is preferred over ΛCDM and $wCDM$ models of the universe.

Bibliography

[1] T. Padmanabhan. Theoretical Astrophysics: Volume 3, Galaxies and Cosmology Ch-3 ,*Cambridge University Press*, 2000

[2] Melia,Fulvio. The cosmic space-time. ,*eprint arXiv:1205.2713*, 2012.

[3] P. J. E. Peebles. The Principles of Physical Cosmology Ch-23 ,*Princeton University Press*, 1993

[4] Felten, J. E.; Gould, R. J.; Stein, W. A.; Woolf, N. J. X-Rays from the Coma Cluster of Galaxies, *Astrophysical Journal*,**vol. 146**, p.955-958, Dec 1966

[5] Craig L. Sarazin. X-ray Emission from Clusters of Galaxies ,*Cambridge Astrophysics Series, Cambridge: Cambridge University Press*, 1988.

[6] Cavaliere, A.; Fusco-Femiano, R. X-rays from hot plasma in clusters of galaxies ,*Astronomy and Astrophysics*, **vol 49**, 137-144, May 1976.

[7] Fixsen, D. J.; Cheng, E. S.; Gales, J. M.; Mather, J. C.; Shafer, R. A.; Wright, E. L. The Cosmic Microwave Background Spectrum from the Full COBE FIRAS Data Set ,*Astrophysical Journal*, **vol 473**, p.576, Dec 1996.

[8] Kenneth P. Burnham,David R. Anderson. Model Selection and Multimodel Inference: A Practical Information-Theoretic Approach,Second Edition ,*Springer*2002

[9] Jun-Jie Wei,Xue-Feng Wu, Fulvio Melia Cosmological tests using the angular size of galaxy clusters, *Mon. Not. R. Astron. Soc.*, **447**, 479-485, 2015.

[10] George B Arfken, Hans J Weber. Mathematical Methods for Physicists, *Sixth Ed.Elsevier Academic Press* , 2005

[11] Shi K., Huang Y. F., Lu T. A comprehensive comparison of cosmological models from the latest observational data, *Mon. Not. R. Astron. Soc.*, **426**, 2452-2462, 2012.

[12] Akaike H. Information theory and an extension of the maximum likelihood principle, *Second International Symposium on Information Theory*, pp. 267-281, 1973

[13] Gurvits, L. I.; Kellermann, K. I.; Frey, S. The "angular size - redshift" relation for compact radio structures in quasars and radio galaxies, *Astronomy and Astrophysics*, **vol 42**, p.378-388, Feb 1999.

[14] McIntosh, Daniel H.; Bell, Eric F.; Rix, Hans-Walter; Wolf, Christian; Heymans, Catherine; Peng, Chien Y.; Somerville, Rachel S.; Barden, Marco; Beckwith, Steven V. W.; Borch, Andrea; Caldwell, John A. R.; Häußler, Boris; Jahnke, Knud; Jogee, Shardha; Meisenheimer, Klaus; Sánchez, Sebastián F.; Wisotzki, Lu. The Evolution of Early-Type Red Galaxies with the GEMS Survey: Luminosity-Size and Stellar Mass-Size Relations Since z=1, *Astrophysical Journal*, **vol 632**, p.191-209, Oct 2005.

[15] Massimiliano Bonamente, Marshall K. Joy Samuel J. LaRoque, John E. Carlstrom, Erik D. Reese, and Kyle S. Dawson Determination of the Cosmic Distance Scale from Sunyaev-Zel'dovich Effect and Chandra X-Ray Measurements of High-Redshift Galaxy Clusters, *Astrophysical Journal*, **vol 647**, p.25-54, Aug 2006.

[16] Erik D. Reese, John E. Carlstrom,Marshall Joy, Joseph J. Mohr, Laura Grego and William L. Holzapfel: Determining the Cosmic Distance Scale from Interferometric Measurements of the Sunyaev Zel'dovich Effect, *Astrophysical Journal*, **vol 581**,p.53–85, Dec 2002.

[17] Elisabetta De Filippis, Mauro Sereno, Mark W. Bautz, and Giuseppe Longo. Measuring thr Three-Dimensional Structure of Galaxy Clusters. I. Application to a Sample of 25 Clusters, *Astrophysical Journal*, **vol 625**, p:108–120, May, 2005

[18] John C. Raymond and Barham W. Smith. Soft X-Ray Spectrum of a Hot Plasma, *Astrophysical Journal*, **vol 35**, p:419–439, Dec, 1977

[19] Reese, Erik D.; Mohr, Joseph J.; Carlstrom, John E.; Joy, Marshall; Grego, Laura; Holder, Gilbert P.; Holzapfel, William L.; Hughes, John P.; Patel, Sandeep K.; Donahue, Megan. Sunyaev-Zeldovich Effect-derived Distances to the High-Redshift Clusters MS 0451.6-0305 and CL 0016+16, *The Astrophysical Journal* **Vol 533**,pp. 38-49. April, 2000

[20] Ashutosh Tripathi,Archana Sangwan,H. K. Jassal.Dark energy equation of state parameter and its evolution at low redshift, *arXiv:1611.01899v3*, Mar,2017

[21] C. Ngeow , S. Kanbur. The Hubble Constant from Type Ia Supernova Calibrated with the Linear and Non-Linear Cepheid Period-Luminosity Relation, *Astrophysical Journal*, **vol.642**,p:29-32, Mar, 2006